

**The protonmotive force and respiratory control:
Building blocks of mitochondrial physiology
Part 1.**

http://www.mitoeagle.org/index.php/MitoEAGLE_preprint_2017-09-21

Preprint version 18 (2017-11-21)

MitoEAGLE Network

Corresponding author: Gnaiger E

Contributing co-authors

Ahn B, Alves MG, Amati F, Aral C, Arandarčikaitė O, Åsander Frostner E, Bailey DM, Bastos Sant'Anna Silva AC, Battino M, Beard DA, Ben-Shachar D, Bishop D, Breton S, Brown GC, Brown RA, Buettner GR, Calabria E, Cardoso LHD, Carvalho E, Casado Pinna M, Cervinkova Z, Chang SC, Chicco AJ, Coen PM, Collins JL, Crisóstomo L, Davis MS, Dias T, Distefano G, Doerrier C, Drahotka Z, Ehinger J, Elmer E, Endlicher R, Fell DA, Ferko M, Ferreira JCB, Filipovska A, Fisar Z, Fisher J, Garcia-Roves PM, Garcia-Souza LF, Genova ML, Gonzalo H, Goodpaster BH, Gorr TA, Grefte S, Han J, Harrison DK, Hellgren KT, Hernansanz P, Holland O, Hoppel CL, Houstek J, Iglesias-Gonzalez J, Irving BA, Iyer S, Jackson CB, Jansen-Dürr P, Jespersen NR, Jha RK, Kaambre T, Kane DA, Kappler L, Karabatsiakakis A, Keijzer J, Keppner G, Komlodi T, Kopitar-Jerala N, Krako Jakovljevic N, Kuang J, Kucera O, Labieniec-Watala M, Lai N, Laner V, Larsen TS, Lee HK, Lemieux H, Lerfall J, Lucchinetti E, MacMillan-Crow LA, Makrecka-Kuka M, Meszaros AT, Michalak S, Moiso N, Molina AJA, Montaigne D, Moore AL, Moreira BP, Mracek T, Muntane J, Muntean DM, Murray AJ, Nemeš M, Newsom S, Nozickova K, O'Gorman D, Oliveira PF, Oliveira PJ, Orynbayeva Z, Pak YK, Palmeira CM, Patel HH, Pecina P, Pereira da Silva Grilo da Silva F, Pesta D, Petit PX, Pichaud N, Pirkmajer S, Porter RK, Pranger F, Prochownik EV, Puurand M, Radenkovic F, Reboredo P, Renner-Sattler K, Robinson MM, Rohlena J, Røslund GV, Rossiter HB, Rybacka-Mossakowska J, Salvadego D, Scatena R, Schartner M, Scheibye-Knudsen M, Schilling JM, Schlattner U, Schoenfeld P, Scott GR, Shabalina IG, Shevchuk I, Siewiera K, Singer D, Sobotka O, Spinazzi M, Stankova P, Stier A, Stocker R, Sumbalova Z, Suravajhala P, Tanaka M, Tandler B, Tepp K, Tomar D, Towheed A, Tretter L, Trivigno C, Tronstad KJ, Trougakos IP, Tyrrell DJ, Urban T, Velika B, Vendelin M, Vercesi AE, Victor VM, Villena JA, Wagner BA, Ward ML, Watala C, Wei YH, Wieckowski MR, Wohlwend M, Wolff J, Wuest RCI, Zaugg K, Zaugg M, Zorzano A

Supporting co-authors:

Bakker BM, Bernardi P, Boetker HE, Borsheim E, Borutaitė V, Bouitbir J, Calbet JA, Chaurasia B, Clementi E, Coker RH, Collin A, Das AM, De Palma C, Dubouchaud H, Duchon MR, Durham WJ, Dyrstad SE, Engin AB, Fornaro M, Gan Z, Garland KD, Garten A, Gourlay CW, Granata C, Haas CB, Haavik J, Haendeler J, Hand SC, Hepple RT, Hickey AJ, Hoel F, Kainulainen H, Khamoui AV, Klingenspor M, Koopman WJH, Kowaltowski AJ, Krajcova A, Lenaz G, Malik A, Markova M, Mazat JP, Menze MA, Methner A, Muntané J, Neuzil J, Oliveira MT, Pallotta ML, Parajuli N, Pettersen IKN, Porter C, Pulinilkunnil T, Ropelle ER, Salin K, Sandi C, Sazanov LA, Silber AM, Skolik R, Smenes BT, Soares FAA, Sokolova I, Sonkar VK, Swerdlow RH, Szabo I, Trifunovic A, Thyfault JP, Valentine JM, Vieyra A, Votion DM, Williams C

Updates:

http://www.mitoeagle.org/index.php/MitoEAGLE_preprint_2017-09-21

Correspondence: Gnaiger E

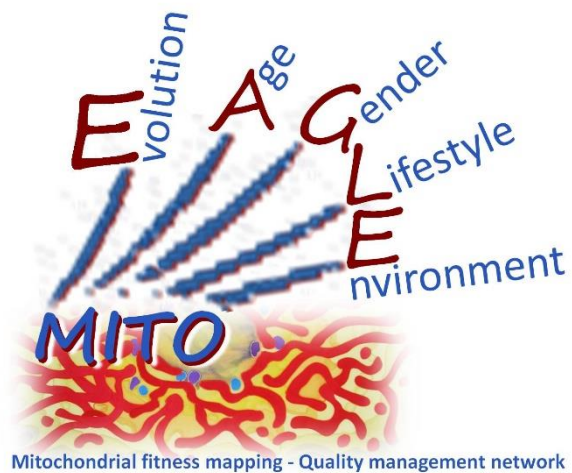
Department of Visceral, Transplant and Thoracic Surgery, D. Swarovski Research
Laboratory, Medical University of Innsbruck, Innrain 66/4, A-6020 Innsbruck, Austria

Email: erich.gnaiger@i-med.ac.at

Tel: +43 512 566796, Fax: +43 512 566796 20

This manuscript on 'The protonmotive force and respiratory control' is a position statement in the frame of COST Action CA15203 MitoEAGLE. The list of co-authors evolved beyond **phase 1** in the **bottom-up** spirit of COST (phase 1 versions 1-44).

This is an open invitation to scientists and students to join as co-authors, to provide a balanced view on mitochondrial respiratory control, a fundamental introductory presentation of the concept of the protonmotive force, and a consensus statement on reporting data of mitochondrial respiration in terms of metabolic flows and fluxes.



Phase 2: MitoEAGLE preprint (Versions 01 – 15): We continue to invite comments and suggestions, particularly if you are an **early career investigator adding an open future-oriented perspective**, or an **established scientist providing a balanced historical basis**. Your critical input into the quality of the manuscript will be most welcome, improving our aims to be educational, general, consensus-oriented, and practically helpful for students working in mitochondrial respiratory physiology.

Phase 3 (2017-11-11) Print version for MiP2017 and MitoEAGLE workshop in Hradec Kralove:

» http://www.mitoeagle.org/index.php/MiP2017_Hradec_Kralove_CZ

Discussion of manuscript submission to a preprint server, such as BioRxiv; invite further opinion leaders: To join as a co-author, please feel free to focus on a particular section in terms of direct input and references, contributing to the scope of the manuscript from the perspective of your expertise. Your comments will be largely posted on the discussion page of the MitoEAGLE preprint website.

If you prefer to submit comments in the format of a referee's evaluation rather than a contribution as a co-author, I will be glad to distribute your views to the updated list of co-authors for a balanced response. We would ask for your consent on this open bottom-up policy.

Phase 4: Journal submission. We plan a series of follow-up reports by the expanding MitoEAGLE Network, to increase the scope of recommendations on harmonization and facilitate global communication and collaboration. Further discussions: MitoEAGLE Working Group Meetings, various conferences (EBEC 2018 in Budapest).

I thank you in advance for your feedback.

With best wishes,

Erich Gnaiger

Chair Mitochondrial Physiology Society - <http://www.mitophysiology.org>

Chair COST Action MitoEAGLE - <http://www.mitoeagle.org>

103	Contents
104	1. Introduction
105	2. Respiratory coupling states in mitochondrial preparations
106	Mitochondrial preparations
107	2.1. <i>Three coupling states of mitochondrial preparations and residual oxygen consumption</i>
108	Coupling control states and respiratory capacities
109	Kinetic control
110	Phosphorylation, P \gg
111	LEAK, OXPHOS, ET, ROX
112	2.2. <i>Coupling states and respiratory rates</i>
113	2.3. <i>Classical terminology for isolated mitochondria</i>
114	States 1-5
115	3. The protonmotive force and proton flux
116	3.1. <i>Electric and chemical partial forces versus electrical and chemical units</i>
117	Faraday constant
118	Electric part of the protonmotive force
119	Chemical part of the protonmotive force
120	3.2. <i>Definitions</i>
121	Control and regulation
122	Respiratory control and response
123	Respiratory coupling control
124	Pathway control states
125	The steady-state
126	3.3. <i>Forces and fluxes in physics and thermodynamics</i>
127	Vectorial and scalar forces, and fluxes
128	Coupling
129	Coupled versus bound processes
130	4. Normalization: fluxes and flows
131	4.1. <i>Flux per chamber volume</i>
132	4.2. <i>System-specific and sample-specific normalization</i>
133	Extensive quantities
134	Size-specific quantities
135	Molar quantities
136	Flow per system, I
137	Size-specific flux, J
138	Sample concentration, C_{mX}
139	Mass-specific flux, J_{mX,O_2}
140	Number concentration, C_{NX}
141	Flow per sample entity, I_{X,O_2}
142	4.3. <i>Normalization for mitochondrial content</i>
143	Mitochondrial concentration, C_{mte} , and mitochondrial markers
144	Mitochondria-specific flux, J_{mte,O_2}
145	4.4. <i>Conversion: units and normalization</i>
146	4.5. <i>Conversion: oxygen, proton and ATP flux</i>
147	5. Conclusions
148	6. References
149	

150 **Abstract** Clarity of concept and consistency of nomenclature are key trademarks of a research
 151 field. These trademarks facilitate effective transdisciplinary communication, education, and
 152 ultimately further discovery. As the knowledge base and importance of mitochondrial
 153 physiology to human health expand, the necessity for harmonizing nomenclature concerning
 154 mitochondrial respiratory states and rates has become increasingly apparent. Peter Mitchell's
 155 chemiosmotic theory establishes the links between electrical and chemical components of
 156 energy transformation and coupling in oxidative phosphorylation. This unifying concept of the
 157 protonmotive force provides the framework for developing a consistent nomenclature for
 158 mitochondrial physiology and bioenergetics. Herein, we follow IUPAC guidelines on general
 159 terms of physical chemistry, extended by the concepts of open systems and irreversible
 160 thermodynamics. We align the nomenclature of classical bioenergetics on respiratory states
 161 with a concept-driven constructive terminology to address the meaning of each respiratory state.
 162 Furthermore, we suggest uniform standards for the evaluation of respiratory states that will
 163 ultimately support the development of databases of mitochondrial respiratory function in
 164 species, tissues and cells studied under diverse physiological and experimental conditions. In
 165 this position statement, in the frame of COST Action MitoEAGLE, we endeavour to provide a
 166 balanced view on mitochondrial respiratory control, a fundamental introductory presentation of
 167 the concept of the protonmotive force, and a critical discussion on reporting data of
 168 mitochondrial respiration in terms of metabolic flows and fluxes.

169
 170 *Keywords:* Mitochondrial respiratory control, coupling control, mitochondrial
 171 preparations, protonmotive force, chemiosmotic theory, oxidative phosphorylation, OXPHOS,
 172 efficiency, electron transfer, ET; proton leak, LEAK, residual oxygen consumption, ROX, State
 173 2, State 3, State 4, normalization, flow, flux
 174

175 **Box 1:**

176 **In brief:**

177 **mitochondria**
 178 **and Bioblasts**

- Does the public expect biologists to understand Darwin's theory of evolution?
- Do students expect that researchers of bioenergetics can explain Mitchell's theory of chemiosmotic energy transformation?

181 **Mitochondria** were described by Richard Altmann (1894) as 'bioblasts', which include not
 182 only the mitochondria as presently defined, but also symbiotic and free-living bacteria. The
 183 word 'mitochondrium' (Greek mitos: thread; chondros: granule) was introduced by Carl Benda
 184 (1898). Mitochondria are the oxygen-consuming electrochemical generators which evolved
 185 from endosymbiotic bacteria (Margulis 1970; Lane 2005).

186 We now recognize mitochondria as dynamic organelles with a double membrane that are
 187 contained within eukaryotic cells. The mitochondrial inner membrane (mtIM) shows dynamic
 188 tubular to disk-shaped cristae that separate the mitochondrial matrix, *i.e.* the internal
 189 mitochondrial compartment, and the intermembrane space; the latter being enclosed by the
 190 mitochondrial outer membrane (mtOM). Mitochondria are the structural and functional
 191 elemental units of cell respiration. Cell respiration is the consumption of oxygen by electron
 192 transfer coupled to electrochemical proton translocation across the mtIM. In the process of
 193 oxidative phosphorylation (OXPHOS), the reduction of O₂ is electrochemically coupled to the
 194 transformation of energy in the form of adenosine triphosphate (ATP; Mitchell 1961, 2011).
 195 These powerhouses of the cell contain the machinery of the OXPHOS-pathway, including
 196 transmembrane respiratory complexes (*i.e.* proton pumps with FMN, Fe-S and cytochrome *b*,
 197 *c*, *aa*₃ redox systems); alternative dehydrogenases and oxidases; the coenzyme ubiquinone (Q);
 198 ATP synthase; the enzymes of the tricarboxylic acid cycle and the fatty acid oxidation enzymes;
 199 transporters of ions, metabolites and co-factors; and mitochondrial kinases related to energy
 200 transfer pathways. The mitochondrial proteome comprises over 1,200 proteins
 201 (MITOCARTA), mostly encoded by nuclear DNA (nDNA), with a variety of functions, many

202 of which are relatively well known (*e.g.* apoptosis-regulating proteins), while others are still
203 under investigation, or need to be identified (*e.g.* alanine transporter).

204 Mitochondria typically maintain several copies of their own genome (hundred to
205 thousands per cell; Cummins 1998), which is almost exclusively maternally inherited (White *et*
206 *al.* 2008) and known as mitochondrial DNA (mtDNA). One exception to strictly maternal
207 inheritance in animals is found in bivalves (Breton *et al.* 2007). mtDNA is 16.5 kB in length,
208 contains 13 protein-coding genes for subunits of the transmembrane respiratory Complexes CI,
209 CIII, CIV and ATP synthase, and also encodes 22 tRNAs and the mitochondrial 16S and 12S
210 rRNA. The mitochondrial genome is both regulated and supplemented by nuclear-encoded
211 mitochondrial targeted proteins. Evidence has accumulated that additional gene content is
212 encoded in the mitochondrial genome, *e.g.* microRNAs, piRNA, smithRNAs, repeat associated
213 RNA, and even additional proteins (Duarte *et al.* 2014; Lee *et al.* 2015; Cobb *et al.* 2016).

214 The mtIM contains the non-bilayer phospholipid cardiolipin, which is not present in any
215 other eukaryotic cellular membrane. Cardiolipin promotes the formation of respiratory
216 supercomplexes, which are supramolecular assemblies based upon specific, though dynamic,
217 interactions between individual respiratory complexes (Greggio *et al.* 2017; Lenaz *et al.* 2017).
218 Membrane fluidity is an important parameter influencing functional properties of proteins
219 incorporated in the membranes (Waczulikova *et al.* 2007). There is a constant crosstalk between
220 mitochondria and the other cellular components, maintaining cellular mitostasis through
221 regulation at both the transcriptional and post-translational level, and through cell signalling
222 including proteostatic (*e.g.* the ubiquitin-proteasome and autophagy-lysosome pathways) and
223 genome stability modules throughout the cell cycle or even cell death, contributing to
224 homeostatic regulation in response to varying energy demands and stress (Quiros *et al.* 2016).
225 In addition to mitochondrial movement along the microtubules, mitochondrial morphology can
226 change in response to the energy requirements of the cell via processes known as fusion and
227 fission, through which mitochondria can communicate within a network, and in response to
228 intracellular stress factors causing swelling and ultimately permeability transition.

229 Mitochondrial dysfunction is associated with a wide variety of genetic and degenerative
230 diseases. Robust mitochondrial function is supported by physical exercise and caloric balance,
231 and is central for sustained metabolic health throughout life. Therefore, a more consistent
232 presentation of mitochondrial physiology will improve our understanding of the etiology of
233 disease, the diagnostic repertoire of mitochondrial medicine, with a focus on protective
234 medicine, lifestyle and healthy aging.

235 Abbreviation: mt, as generally used in mtDNA. Mitochondrion is singular and
236 mitochondria is plural.

237 *‘For the physiologist, mitochondria afforded the first opportunity for an experimental*
238 *approach to structure-function relationships, in particular those involved in active transport,*
239 *vectorial metabolism, and metabolic control mechanisms on a subcellular level’* (Ernster and
240 Schatz 1981).

241

242 **1. Introduction**

243 Mitochondria are the powerhouses of the cell with numerous physiological, molecular,
244 and genetic functions (**Box 1**). Every study of mitochondrial function and disease is faced with
245 **E**volution, **A**ge, **G**ender and sex, **L**ifestyle, and **E**nvironment (EAGLE) as essential background
246 conditions intrinsic to the individual patient or subject, cohort, species, tissue and to some extent
247 even cell line. As a large and highly coordinated group of laboratories and researchers, the
248 mission of the global MitoEAGLE Network is to generate the necessary scale, type, and quality
249 of consistent data sets and conditions to address this intrinsic complexity. Harmonization of
250 experimental protocols and implementation of a quality control and data management system
251 is required to interrelate results gathered across a spectrum of studies and to generate a
252 rigorously monitored database focused on mitochondrial respiratory function. In this way,

253 researchers within the same and across different disciplines will be positioned to compare their
254 findings to an agreed upon set of clearly defined and accepted international standards.

255 Reliability and comparability of quantitative results depend on the accuracy of
256 measurements under strictly-defined conditions. A conceptually defined framework is also
257 required to warrant meaningful interpretation and comparability of experimental outcomes
258 carried out by research groups at different institutes. With an emphasis on quality of research,
259 collected data can be useful far beyond the specific question of a particular experiment.
260 Enabling meta-analytic studies is the most economic way of providing robust answers to
261 biological questions (Cooper *et al.* 2009). Vague or ambiguous jargon can lead to confusion
262 and may relegate valuable signals to wasteful noise. For this reason, measured values must be
263 expressed in standardized units for each parameter used to define mitochondrial respiratory
264 function. Standardization of nomenclature and definition of technical terms is essential to
265 improve the awareness of the intricate meaning of a divergent scientific vocabulary, for
266 documentation and integration into databases in general, and quantitative modelling in
267 particular (Beard 2005). The focus on the protonmotive force, coupling states, and fluxes
268 through metabolic pathways of aerobic energy transformation in mitochondrial preparations is
269 a first step in the attempt to generate a harmonized and conceptually-oriented nomenclature in
270 bioenergetics and mitochondrial physiology. Coupling states of intact cells and respiratory
271 control by fuel substrates and specific inhibitors of respiratory enzymes will be reviewed in
272 subsequent communications.

273

274 **2. Respiratory coupling states in mitochondrial preparations**

275 *‘Every professional group develops its own technical jargon for talking about*
276 *matters of critical concern ... People who know a word can share that idea with*
277 *other members of their group, and a shared vocabulary is part of the glue that holds*
278 *people together and allows them to create a shared culture’ (Miller 1991).*

279 **Mitochondrial preparations** are defined as either isolated mitochondria, or tissue and
280 cellular preparations in which the barrier function of the plasma membrane is disrupted. The
281 plasma membrane separates the cytosol, nucleus, and organelles (the intracellular
282 compartment) from the environment of the cell. The plasma membrane consists of a lipid
283 bilayer, embedded proteins, and attached organic molecules that collectively control the
284 selective permeability of ions, organic molecules, and particles across the cell boundary. The
285 intact plasma membrane, therefore, prevents the passage of many water-soluble mitochondrial
286 substrates, such as succinate or adenosine diphosphate (ADP), that are required for the analysis
287 of respiratory capacity at kinetically-saturating concentrations, thus limiting the scope of
288 investigations into mitochondrial respiratory function in intact cells. The cholesterol content of
289 the plasma membrane is high compared to mitochondrial membranes. Therefore, mild
290 detergents, such as digitonin and saponin, can be applied to selectively permeabilize the plasma
291 membrane by interaction with cholesterol and allow free exchange of cytosolic components
292 with ions and organic molecules of the immediate cell environment, while maintaining the
293 integrity and localization of organelles, cytoskeleton, and the nucleus. Application of optimum
294 concentrations of these mild detergents leads to the complete loss of cell viability, tested by
295 nuclear staining and washout of cytosolic marker enzymes such as lactate dehydrogenase, while
296 mitochondrial function remains intact, as shown by an unaltered respiration rate of isolated
297 mitochondria after the addition of such low concentrations of digitonin and saponin. In addition
298 to mechanical permeabilization during homogenization of fresh tissue, either detergents (*e.g.*
299 saponin) or toxins may be applied to ensure permeabilization of all cells. Crude homogenate
300 and cells permeabilized in the respiration chamber contain all components of the cell at highly
301 diluted concentrations. All mitochondria are retained in chemically-permeabilized
302 mitochondrial preparations and crude tissue homogenates. In the preparation of isolated
303 mitochondria, the cells or tissues are homogenized, and the mitochondria are separated from

304 other cell fractions and purified by differential centrifugation, entailing the loss of a fraction of
 305 mitochondria, *i.e.* a mitochondrial yield in the range of 30% to 80%. Maximization of the purity
 306 of isolated mitochondria may compromise not only the mitochondrial yield but also the
 307 structural and functional integrity. Therefore, protocols for isolation of mitochondria need to
 308 be optimized according to the relevant questions addressed in a study. The mitochondrial yield
 309 and experimental criteria for evaluation of purity versus integrity should be reported. The term
 310 mitochondrial preparation does not include further fractionation of mitochondrial components,
 311 as well as submitochondrial particles.

312

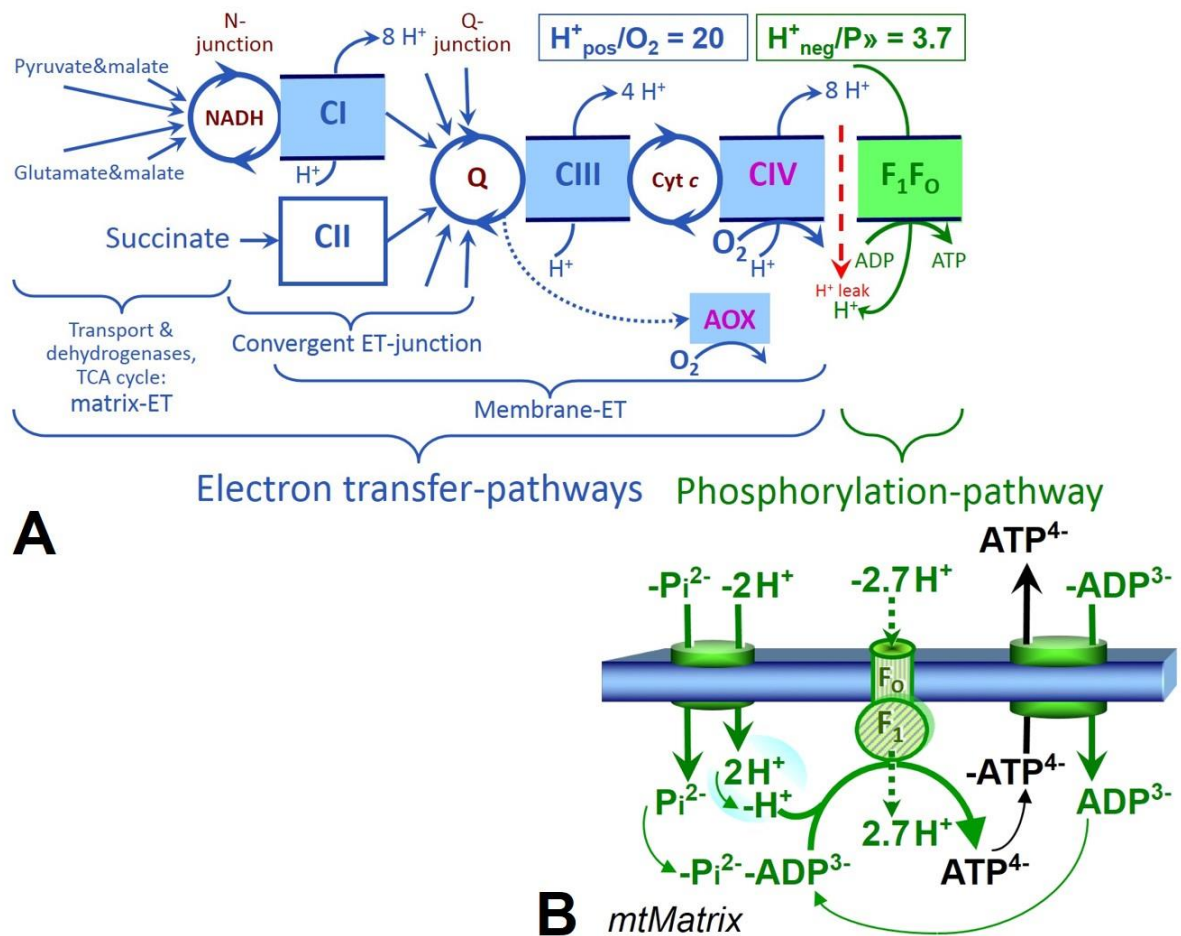
313 *2.1. Three coupling states of mitochondrial preparations and residual oxygen consumption*

314 **Respiratory capacities in coupling control states:** To extend the classical nomenclature
 315 on mitochondrial coupling states (Section 2.4) by a concept-driven terminology that
 316 incorporates explicit information on the nature of the respiratory states, the terminology must
 317 be general and not restricted to any particular experimental protocol or mitochondrial
 318 preparation (Gnaiger 2009). We focus primarily on the conceptual ‘why’, along with
 319 clarification of the experimental ‘how’. In the following section, the concept-driven
 320 terminology is explained and coupling states are defined. We define respiratory capacities,
 321 comparable to channel capacity in information theory (Schneider 2006), as the upper bound of
 322 the rate of respiration measured in defined coupling control states and electron transfer-pathway
 323 (ET-pathway) control states. To provide a diagnostic reference for respiratory capacities of core
 324 energy metabolism, the capacity of *oxidative phosphorylation*, OXPHOS, is measured at
 325 kinetically-saturating concentrations of ADP and inorganic phosphate, P_i . The *oxidative* ET-
 326 capacity reveals the limitation of OXPHOS-capacity mediated by the *phosphorylation*-
 327 pathway. The ET- and phosphorylation-pathways comprise coupled segments of the OXPHOS-
 328 pathway. ET-capacity is measured as noncoupled respiration by application of *external*
 329 *uncouplers*. The contribution of *intrinsically uncoupled* oxygen consumption is most easily
 330 studied in the absence of ADP, *i.e.* by not stimulating phosphorylation, or by inhibition of the
 331 phosphorylation-pathway. The corresponding states are collectively classified as LEAK-states,
 332 when oxygen consumption compensates mainly for the proton leak (**Table 1**). Different
 333 coupling states are induced by: (1) adding ADP or P_i ; (2) inhibiting the phosphorylation-
 334 pathway; and (3) uncoupler titrations, while maintaining a defined ET-pathway state with
 335 constant fuel substrates and inhibitors of specific branches of the ET-pathway (**Fig. 1**).

336 **Kinetic control:** Coupling control states are established in the study of mitochondrial
 337 preparations to obtain reference values for various output variables. Physiological conditions *in*
 338 *vivo* deviate from these experimentally obtained states. Since kinetically-saturating
 339 concentrations, *e.g.* of ADP or oxygen, may not apply to physiological intracellular conditions,
 340 relevant information is obtained in studies of kinetic responses to conditions intermediate
 341 between the LEAK state at zero [ADP] and the OXPHOS-state at saturating [ADP], or of
 342 respiratory capacities in the range between kinetically-saturating [O_2] and anoxia (Gnaiger
 343 2001).

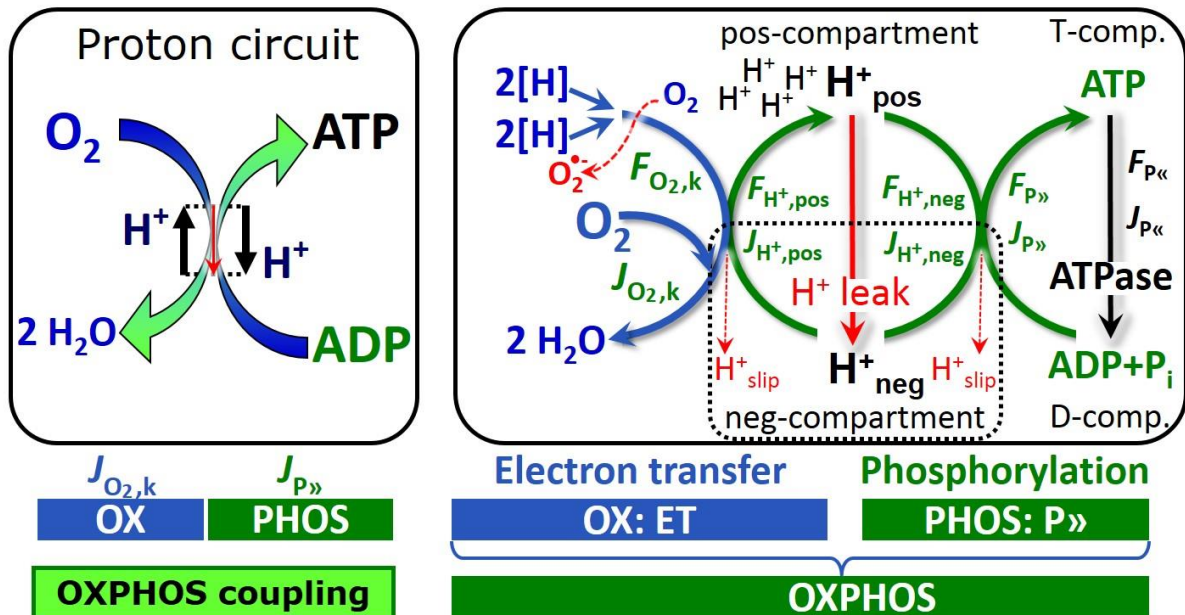
344 **Specification of dose of biochemical additions:** Nominal concentrations of substrates,
 345 uncouplers, inhibitors, and other biochemical reagents titrated to dissect mitochondrial function
 346 are usually reported as initial amount of substance concentration [$\text{mol}\cdot\text{L}^{-1}$] in the incubation
 347 medium. When aiming at the measurement of kinetically saturated processes such as OXPHOS
 348 capacities, the concentrations for substrates can be chosen in light of the K_m . In the case of
 349 hyperbolic kinetics, only 80% of maximum respiratory capacity is obtained at a substrate
 350 concentration of four times the K_m , whereas substrate concentrations of 9, 19 and 49 times the
 351 K_m are theoretically required for reaching 90%, 95% or 98% of the maximal rate (Gnaiger
 352 2001). Other reagents are chosen to inhibit or alter some process. The amount of these tools in
 353 an experimental incubation is selected to maximize effect, yet not lead to unacceptable off-
 354 target consequences that would adversely affect the data being sought. Specifying the amount

355 of substance in an incubation as nominal concentration in the aqueous incubation medium can
 356 be ambiguous (Doskey *et al.* 2015), particularly when lipid-soluble substances (oligomycin;
 357 uncouplers) or cations (TPP⁺; fluorescent dyes such as safranin, TMRM) are applied which
 358 accumulate in biological membranes or in the mitochondrial matrix, respectively. For example,
 359 a dose of digitonin of 8 fmol·cell⁻¹ (10 μg·10⁻⁶ cells) is optimal for permeabilization of
 360 endothelial cells, and the concentration in the incubation medium has to be adjusted according
 361 to the cell density applied (Doerrier *et al.* 2017). Generally, dose/exposure can be specified per
 362 unit of biological sample, *i.e.* (nominal moles of xenobiotic)/(number of cells) [mol·cell⁻¹] or,
 363 as appropriate, per mass of biological sample [mol·g⁻¹]. This approach to specification of
 364 dose/exposure provides a scalable parameter that can be used to design experiments, help
 365 interpret a wide variety of experimental results, and provide absolute information that allows
 366 researchers worldwide to make the most use of published data (Doskey *et al.* 2015).
 367



368
 369 **Fig. 1. The oxidative phosphorylation-pathway, OXPHOS-pathway.** (A) Electron transfer,
 370 ET, coupled to phosphorylation. ET-pathways converge at the N- and Q-junction, as shown for
 371 the NADH- and succinate-pathway; additional arrows indicate electron entry into the Q-
 372 junction through electron transferring flavoprotein, glycerophosphate dehydrogenase, dihydro-
 373 orotate dehydrogenase, choline dehydrogenase, and sulfide-ubiquinone oxidoreductase. The
 374 branched pathway of oxygen consumption by alternative quinol oxidase (AOX) is indicated by
 375 the dotted arrow. The H⁺_{pos}/O₂ ratio is the outward proton flux from the matrix space to the
 376 positively charged compartment, divided by catabolic O₂ flux in the NADH-pathway. The
 377 H⁺_{neg}/P» ratio is the inward proton flux from the inter-membrane space to the negatively
 378 charged matrix space, divided by the flux of phosphorylation of ADP to ATP. Due to proton
 379 leak and slip these are not fixed stoichiometries. (B) Phosphorylation-pathway catalyzed by the
 380 F₁F₀ ATP synthase, adenine nucleotide translocase, and inorganic phosphate transporter. The

381 H^+_{neg}/P_{\gg} stoichiometry is the sum of the coupling stoichiometry in the ATP synthase reaction
 382 ($-2.7 H^+$ from the intermembrane space, $2.7 H^+$ to the matrix) and the proton balance in the
 383 translocation of ADP^{2-} , ATP^{3-} and P_i^{2-} . See Eqs. 5 and 6 for further explanation. Modified from
 384 (A) Lemieux *et al.* (2017) and (B) Gnaiger (2014).
 385



386
 387 **Fig. 2. The proton circuit and coupling in oxidative phosphorylation (OXPHOS).** Oxygen
 388 flux, $J_{O_2,k}$, through the catabolic ET-pathway k is coupled to flux through the phosphorylation-
 389 pathway of ADP to ATP, $J_{P_{\gg}}$, by the proton pumps of the ET-pathway, driving the outward
 390 proton flux, $J_{H^+,pos}$, and generating the output protonmotive force, $F_{H^+,pos}$. ATP synthase is
 391 coupled to inward proton flux, $J_{H^+,neg}$, to phosphorylate $ADP + P_i$ to ATP, driven by the input
 392 protonmotive force, $F_{H^+,neg} = -F_{H^+,pos}$. $2[H]$ indicates the reduced hydrogen equivalents of fuel
 393 substrates that provide the chemical input force, $F_{O_2,k}$ [kJ/mol O_2], of the catabolic reaction k
 394 with oxygen (Gibbs energy of reaction per mole O_2 consumed in reaction k), typically in the
 395 range of -460 to -480 kJ/mol. The output force is given by the phosphorylation potential
 396 difference (ADP phosphorylated to ATP), $F_{P_{\gg}}$, which varies *in vivo* ranging from about 48 to
 397 62 kJ/mol under physiological conditions (Gnaiger 1993a). Fluxes, J_B , and forces, F_B , are
 398 expressed in either chemical units, [$mol \cdot s^{-1} \cdot m^{-3}$] and [$J \cdot mol^{-1}$] respectively, or electrical units,
 399 [$C \cdot s^{-1} \cdot m^{-3}$] and [$J \cdot C^{-1}$] respectively. Fluxes are expressed per volume, V [m^3], of the system. The
 400 system defined by the boundaries (full black line) is not a black box, but is analysed as a
 401 compartmental system. The negative compartment (neg-compartment, enclosed by the dotted
 402 line) is the matrix space, separated from the positive compartment (pos-compartment) by the
 403 mtIM. $ADP + P_i$ and ATP are the substrate- and product-compartments (scalar ADP and ATP
 404 compartments, D-comp. and T-comp.), respectively. Chemical potentials of all substrates and
 405 products involved in the scalar reactions are measured in the pos-compartment for calculation
 406 of the scalar forces $F_{O_2,k}$ and $F_{P_{\gg}} = -F_{P_{\ll}}$ (**Box 2**). Modified from Gnaiger (2014).
 407

408 **Phosphorylation, P \gg :** Phosphorylation in the context of OXPHOS is defined as
 409 phosphorylation of ADP to ATP. On the other hand, the term phosphorylation is used generally
 410 in many different contexts, *e.g.* protein phosphorylation. This justifies consideration of a
 411 symbol more discriminating and specific than P as used in the P/O ratio (phosphate to atomic
 412 oxygen ratio; $O = 0.5 O_2$), where P indicates phosphorylation of ADP to ATP or GDP to GTP.
 413 We propose the symbol P \gg for the endergonic direction of phosphorylation $ADP \rightarrow ATP$, and
 414 likewise the symbol P \ll for the corresponding exergonic hydrolysis $ATP \rightarrow ADP$ (**Fig. 2; Box**
 415 **3**). $J_{P_{\gg}}/J_{O_2,k}$ (P \gg / O_2) is two times the 'P/O' ratio of classical bioenergetics. ATP synthase is the

416 proton pump of the phosphorylation-pathway (**Fig. 1B**). P_{\gg} may also involve substrate-level
 417 phosphorylation as part of the tricarboxylic acid cycle (succinyl-CoA ligase) and
 418 phosphorylation of ADP catalyzed by phosphoenolpyruvate carboxykinase, adenylate kinase,
 419 creatine kinase, hexokinase and nucleoside diphosphate kinase. Kinase cycles are involved in
 420 intracellular energy transfer and signal transduction for regulation of energy flux. In isolated
 421 mammalian mitochondria ATP production catalyzed by adenylate kinase, $2ADP \leftrightarrow ATP +$
 422 AMP , proceeds without fuel substrates in the presence of ADP (Komlódi and Tretter 2017).
 423 The effective P_{\gg}/O_2 ratio is diminished by: (1) the proton leak across the mtIM from low pH in
 424 the positively charged compartment to high pH in the negatively charged compartment; (2)
 425 cycling of other cations; (3) proton slip in the proton pumps when protons are effectively not
 426 pumped; (4) loss of compartmental integrity; and (5) electron leak in the univalent reduction of
 427 oxygen (O_2 ; dioxygen) to superoxide anion radical ($O_2^{\cdot-}$).

428
 429 **LEAK-state (Fig. 3):** The
 430 LEAK-state is defined as a state
 431 of mitochondrial respiration
 432 when O_2 flux mainly
 433 compensates for the proton leak
 434 in the absence of ATP synthesis,
 435 at kinetically-saturating
 436 concentrations of O_2 and
 437 respiratory fuel substrates.
 438 LEAK-respiration is measured to
 439 obtain an indirect estimate of
 440 *intrinsic uncoupling* without
 441 addition of any experimental
 442 uncoupler: (1) in the absence of
 443 adenylates; (2) after depletion of
 444 ADP at maximum ATP/ADP

445 ratio; or (3) after inhibition of the phosphorylation-pathway by inhibitors of ATP synthase, such
 446 as oligomycin, or adenine nucleotide translocase, such as carboxyatractyloside. It is important
 447 to consider adjustment of the nominal concentration of these inhibitors to the density of
 448 biological sample applied, to minimize or avoid inhibitory side-effects exerted on ET-capacity
 449 or even some uncoupling.

450 **Proton leak and uncoupled respiration:** Proton leak is a leak current of protons. Proton
 451 leak is the *uncoupled* process in which protons diffuse across the mtIM in the dissipative
 452 direction of the downhill protonmotive force without coupling to phosphorylation (**Fig. 3**). The
 453 proton leak flux, $J_{H^+,neg,L}$, depends non-linearly on the protonmotive force (Garlid *et al.* 1989;
 454 Divakaruni and Brand 2011), is a property of the mtIM, may be enhanced due to possible
 455 contaminations by free fatty acids, and is physiologically controlled. In particular, inducible
 456 uncoupling mediated by uncoupling protein 1 (UCP1) is physiologically controlled, *e.g.*, in
 457 brown adipose tissue. UCP1 is a member of the mitochondrial carrier family which is involved
 458 in the translocation of protons across the mtIM (Klingenberg 2017). As a consequence of this
 459 effective short-circuit, the protonmotive force diminishes, resulting in stimulation of electron
 460 transfer to oxygen and heat dissipation without phosphorylation of ADP. Mitochondrial injuries
 461 may lead to *dyscoupling* as a pathological or toxicological cause of *uncoupled* respiration, *e.g.*,
 462 as a consequence of opening the permeability transition pore. Dyscoupled respiration is
 463 distinguished from the experimentally induced *noncoupled* respiration in the ET-state. Under
 464 physiological conditions, the proton leak is the dominant contributor to the overall leak current
 465 (Dufour *et al.* 1996).

466

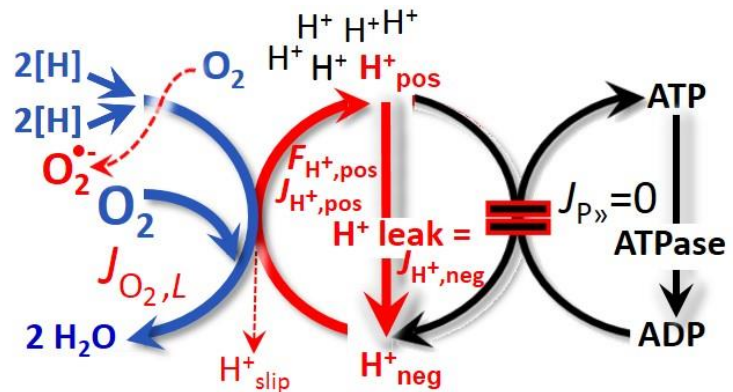


Fig. 3. LEAK-state: Phosphorylation is arrested, $J_{P_{\gg}} = 0$, and oxygen flux, $J_{O_2,L}$, is controlled mainly by the proton leak, $J_{H^+,neg,L}$, at maximum protonmotive force, $F_{H^+,pos}$. See also Fig. 2.

467 **Table 1. Coupling states and residual oxygen consumption in mitochondrial**
 468 **preparations in relation to respiration- and phosphorylation-rate, $J_{O_2,k}$ and $J_{P_{\gg}}$,**
 469 **and protonmotive force, $F_{H^+,pos}$.** Coupling states are established at kinetically-
 470 saturating concentrations of fuel substrates and O_2 .

State	$J_{O_2,k}$	$J_{P_{\gg}}$	$F_{H^+,pos}$	Inducing factors	Limiting factors
LEAK	L ; low, proton leak-dependent respiration	0	max.	Proton leak, slip, and cation cycling	$J_{P_{\gg}} = 0$: (1) without ADP, L_N ; (2) max. ATP/ADP ratio, L_T ; or (3) inhibition of the phosphorylation-pathway, L_{Omy}
OXPHOS	P ; high, ADP-stimulated respiration	max.	high	Kinetically-saturating [ADP] and [P_i]	$J_{P_{\gg}}$ by phosphorylation-pathway; or $J_{O_2,k}$ by ET-capacity
ET	E ; max., noncoupled respiration	0	low	Optimal external uncoupler concentration for max. oxygen flux	$J_{O_2,k}$ by ET-capacity
ROX	R_{ox} ; min., residual O_2 consumption	0	0	$J_{O_2,Rox}$ in non-ET-pathway oxidation reactions	Full inhibition of ET-pathway; or absence of fuel substrates

471
 472
 473

Table 2. Distinction of terms related to coupling.

Term	Respiration	P_{\gg}/O_2	Note
Fully coupled	$P - L$	max.	OXPHOS-capacity corrected for LEAK-respiration (Fig. 6)
Well-coupled	P	high	Phosphorylating respiration with an intrinsic LEAK component (Fig. 4)
Dyscoupled	P	low	Pathologically, toxicologically, environmentally increased uncoupling, mitochondrial dysfunction
Loosely coupled	L	low	Electron leak to superoxide anion radical
Acoupled		0	Electron transfer in mitochondrial fragments without vectorial proton translocation
Uncoupled and decoupled	L	0	Non-phosphorylating intrinsic LEAK-respiration including decoupled and acoupled respiration, without added protonophore (Fig. 3)
Inducibly uncoupled	E	0	By UCP1 or cation (<i>e.g.</i> Ca^{2+}) cycling
Noncoupled	E	0	Non-phosphorylating respiration stimulated to maximum flux at optimum exogenous uncoupler concentration (Fig. 5)

474

475 **Electron leak and loosely coupled respiration:** Superoxide anion radical production by
 476 the electron transfer system leads to a bypass of proton pumps and correspondingly lower P_{\gg}/O_2
 477 ratio, which depends on the actual site of electron leak and the scavenging of hydrogen peroxide
 478 by cytochrome *c*, whereby electrons may re-enter the ETS with proton translocation by CIV.

479 **Proton slip and decoupled respiration:** Proton slip is the *decoupled* process in which
 480 protons are only partially translocated by a proton pump of the ET-pathways and slip back to
 481 the original compartment (Dufour *et al.* 1996). Proton slip can also happen in association with
 482 the ATP-synthase, in which case the proton slips downhill across the pump to the matrix without
 483 contributing to ATP synthesis. In each case, proton slip is a property of the proton pump and
 484 increases with the turnover rate of the pump.

485 **Loss of compartmental integrity and acoupled respiration:** Electron transfer and O_2
 486 consumption proceed without compartmental proton translocation in disrupted mitochondrial
 487 fragments. Such fragments form during mitochondrial isolation, and may not fully fuse to re-
 488 establish structurally intact mitochondria. Loss of mtIM integrity, therefore, is the cause of
 489 acoupled respiration, which is a nonvectorial dissipative process without control by the
 490 protonmotive force.

491 **Cation cycling:** There can be other cation contributors to leak current including calcium
 492 and probably magnesium. Calcium current is balanced by mitochondrial Na/Ca exchange,
 493 which is balanced by Na/H exchange or K/H exchange. This is another effective uncoupling
 494 mechanism different from proton leak and slip.

495 Small differences of terms, *e.g.*, uncoupled, noncoupled, are easily overlooked and may
 496 be erroneously perceived as identical. Even with an attempt at rigorous definition, the common
 497 use of such terms may remain vague (**Table 2**).

498 **OXPHOS-state (Fig. 4):**

500 The OXPHOS-state is defined as
 501 the respiratory state with
 502 kinetically-saturating
 503 concentrations of O_2 , respiratory
 504 and phosphorylation substrates,
 505 and absence of exogenous
 506 uncoupler, which provides an
 507 estimate of the maximal
 508 respiratory capacity in the
 509 OXPHOS-state for any given ET-
 510 pathway state. Respiratory
 511 capacities at kinetically-
 512 saturating substrate
 513 concentrations provide reference
 514 values or upper limits of
 515 performance, aiming at the generation of data sets for comparative purposes. Physiological
 516 activities and effects of substrate kinetics can be evaluated relative to OXPHOS capacities.

517 As discussed previously, 0.2 mM ADP does not fully saturate flux in isolated
 518 mitochondria (Gnaiger 2001; Puchowicz *et al.* 2004); greater ADP concentration is required,
 519 particularly in permeabilized muscle fibres and cardiomyocytes, to overcome limitations by
 520 intracellular diffusion and by the reduced conductance of the mitochondrial outer membrane,
 521 mtOM (Jepihhina *et al.* 2011, Illaste *et al.* 2012, Simson *et al.* 2016), either through interaction
 522 with tubulin (Rostovtseva *et al.* 2008) or other intracellular structures (Birkedal *et al.* 2014). In
 523 permeabilized muscle fibre bundles of high respiratory capacity, the apparent K_m for ADP
 524 increases up to 0.5 mM (Saks *et al.* 1998), indicating that >90% saturation is reached only at
 525 >5 mM ADP. Similar ADP concentrations are also required for accurate determination of

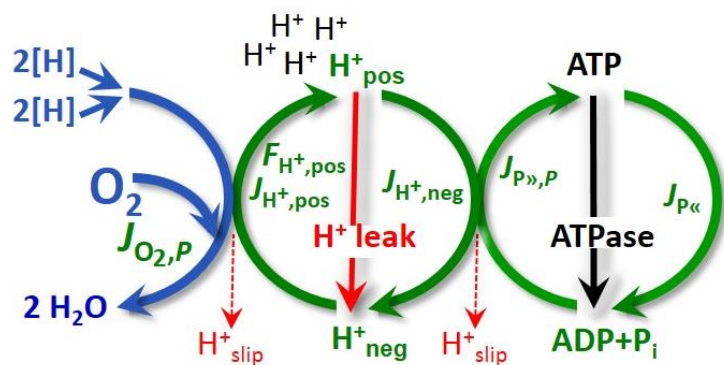


Fig. 4. OXPHOS-state: Phosphorylation, $J_{P_{\gg}}$, is stimulated by kinetically-saturating [ADP] and inorganic phosphate, $[P_i]$, and is supported by a high protonmotive force, $F_{H^+,pos}$. O_2 flux, $J_{O_2,P}$, is well-coupled at a P_{\gg}/O_2 ratio of $J_{P_{\gg},P}/J_{O_2,P}$. See also Fig. 2.

526 OXPHOS-capacity in human clinical cancer samples and permeabilized cells (Klepinin *et al.*
 527 2016; Koit *et al.* 2017). Whereas 2.5 to 5 mM ADP is sufficient to obtain the actual OXPHOS-
 528 capacity in many types of permeabilized tissue and cell preparations, experimental validation
 529 is required in each specific case.

530

531 **Electron transfer-state**
 532 (Fig. 5): The ET-state is defined
 533 as the *noncoupled* state with
 534 kinetically-saturating
 535 concentrations of O₂, respiratory
 536 substrate and optimum
 537 *exogenous* uncoupler
 538 concentration for maximum O₂
 539 flux, as an estimate of oxidative
 540 ET-capacity. Inhibition of
 541 respiration is observed at higher
 542 than optimum uncoupler
 543 concentrations. As a
 544 consequence of the nearly
 545 collapsed protonmotive force, the
 546 driving force is insufficient for
 547 phosphorylation, and $J_{P_{\gg}} = 0$.

548 Besides the three fundamental coupling states of mitochondrial preparations, the
 549 following respiratory state also is relevant to assess respiratory function:

550

551 **ROX:** Residual oxygen consumption (ROX) is defined as O₂ consumption due to
 552 oxidative side reactions remaining after inhibition of ET with rotenone, malonic acid and
 553 antimycin A. Cyanide and azide not only inhibit CIV but several peroxidases which should be
 554 involved in ROX. ROX is not a coupling state but represents a baseline that is used to correct
 555 mitochondrial respiration in defined coupling states. ROX is not necessarily equivalent to non-
 556 mitochondrial respiration, considering oxygen-consuming reactions in mitochondria not related
 557 to ET, such as oxygen consumption in reactions catalyzed by monoamine oxidases (type A and
 558 B), monooxygenases (cytochrome P450 monooxygenases), dioxygenase (sulfur dioxygenase
 559 and trimethyllysine dioxygenase), several hydroxylases, and more. Mitochondrial preparations,
 560 especially those obtained from liver, may be contaminated by peroxisomes. This fact makes the
 561 exact determination of mitochondrial oxygen consumption and mitochondria-associated
 562 generation of reactive oxygen species complicated (Schönfeld *et al.* 2009). The dependence of
 563 ROX-linked oxygen consumption needs to be studied in detail with respect to non-ET enzyme
 564 activities, availability of specific substrates, oxygen concentration, and electron leakage leading
 565 to the formation of reactive oxygen species.

566

567 2.2. Coupling states and respiratory rates

568 It is important to distinguish metabolic *pathways* from metabolic *states* and the
 569 corresponding metabolic *rates*; for example: ET-pathways (Fig. 6), ET-state (Fig. 5), and ET-
 570 capacity, *E*, respectively (Table 1). The protonmotive force is *high* in the OXPHOS-state when
 571 it drives phosphorylation, *maximum* in the LEAK-state of coupled mitochondria, driven by
 572 LEAK-respiration at a minimum back flux of protons to the matrix side, and *very low* in the
 573 ET-state when uncouplers short-circuit the proton cycle (Table 1).

574

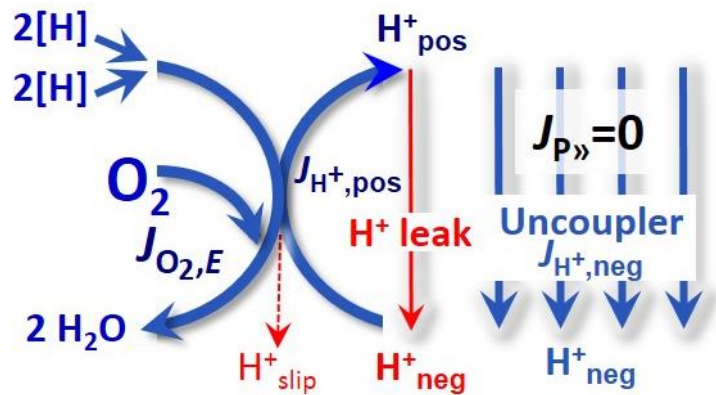
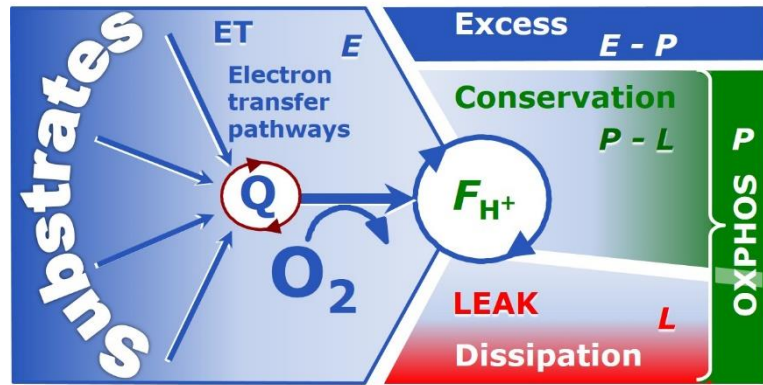


Fig. 5. ET-state: Noncoupled respiration, $J_{O_{2,E}}$, is maximum at optimum exogenous uncoupler concentration and phosphorylation is zero, $J_{P_{\gg}} = 0$. See also Fig. 2.

575 **Fig. 6. Four-compartment**
576 **model of oxidative**

577 **phosphorylation.** Respiratory
578 states (ET, OXPHOS, LEAK)
579 and corresponding rates (E , P , L)
580 are connected by the
581 protonmotive force, F_{H^+} . Electron
582 transfer-capacity, E , is partitioned
583 into (1) dissipative LEAK-
584 respiration, L , when the Gibbs
585 energy change of catabolic O_2



586 consumption is irreversibly lost, (2) net OXPHOS-capacity, $P-L$, with partial conservation of
587 the capacity to perform work, and (3) the excess capacity, $E-P$. Modified from Gnaiger (2014).
588

589 The three coupling states, ET, LEAK and OXPHOS, are shown schematically with the
590 corresponding respiratory rates, abbreviated as E , L and P , respectively (**Fig. 6**). E may exceed
591 or be equal to P , but E cannot theoretically be lower than P . $E < P$ must be discounted as an
592 artefact, which may be caused experimentally by: (1) loss of oxidative capacity during the time
593 course of the respirometric assay, since E is measured subsequently to P ; (2) using insufficient
594 uncoupler concentrations; (3) using high uncoupler concentrations which inhibit ET (Gnaiger
595 2008); (4) high oligomycin concentrations applied for measurement of L before titrations of
596 uncoupler, when oligomycin exerts an inhibitory effect on E . On the other hand, the excess ET-
597 capacity is overestimated if non-saturating [ADP] or [P_i] are used. See State 3 in the next
598 section.

599 $E > P$ is observed in many types of mitochondria, varying between species, tissues and
600 cell types. $E-P$ is the excess ET-capacity pushing the phosphorylation-flux (**Fig. 1B**) to the limit
601 of its *capacity of utilizing* the protonmotive force. Within any type of mitochondria, the
602 magnitude of $E-P$ depends on: (1) the pathway control state with single or multiple electron
603 input into the Q-junction and involvement of three or fewer coupling sites determining the
604 H^+_{pos}/O_2 *coupling stoichiometry* (**Fig. 1A**); and (2) the *biochemical coupling efficiency*
605 expressed as $(E-L)/E$, since an increase of L causes P to increase towards the limit of E . The
606 *excess E-P* capacity, $E-P$, therefore, provides a sensitive diagnostic indicator of specific injuries
607 of the phosphorylation-pathway, under conditions when E remains constant but P declines
608 relative to controls (**Fig. 6**). Substrate cocktails supporting simultaneous convergent electron
609 transfer to the Q-junction for reconstitution of tricarboxylic acid cycle (TCA cycle) function
610 establish pathway control states with high ET-capacity, and consequently increase the
611 sensitivity of the $E-P$ assay.

612 When subtracting L from P , the dissipative LEAK component in the OXPHOS-state may
613 be overestimated. This can be avoided by measuring LEAK-respiration in a state when the
614 protonmotive force is adjusted to its slightly lower value in the OXPHOS-state, *e.g.*, by titration
615 of an ET inhibitor (Divakaruni and Brand 2011). Any turnover-dependent components of
616 proton leak and slip, however, are underestimated under these conditions (Garlid *et al.* 1993).
617 In general, it is inappropriate to use the term *ATP production* or *ATP turnover* for the difference
618 of oxygen consumption measured in states P and L . The difference $P-L$ is the upper limit of the
619 part of OXPHOS-capacity that is freely available for ATP production (corrected for LEAK-
620 respiration) and is fully coupled to phosphorylation with a maximum mechanistic stoichiometry
621 (**Fig. 6**).
622
623

624 2.3. Classical terminology for isolated mitochondria

625 'When a code is familiar enough, it ceases appearing like a code; one forgets that
626 there is a decoding mechanism. The message is identical with its meaning'
627 (Hofstadter 1979).

628 Chance and Williams (1955; 1956) introduced five classical states of mitochondrial respiration
629 and cytochrome redox states. **Table 3** shows a protocol with isolated mitochondria in a closed
630 respirometric chamber, defining a sequence of respiratory states.

631

632

633

634

Table 3. Metabolic states of mitochondria (Chance and Williams, 1956; Table V).

State	[O ₂]	ADP level	Substrate Level	Respiration rate	Rate-limiting substance
1	>0	low	low	slow	ADP
2	>0	high	~0	slow	substrate
3	>0	high	high	fast	respiratory chain
4	>0	low	high	slow	ADP
5	0	high	high	0	oxygen

635

636

637

638

State 1 is obtained after addition of isolated mitochondria to air-saturated isoosmotic/isotonic respiration medium containing inorganic phosphate, but no fuel substrates and no adenylates, *i.e.*, AMP, ADP, ATP.

639

640

641

642

643

644

645

646

647

648

649

650

State 2 is induced by addition of a high concentration of ADP (typically 100 to 300 μ M), which stimulates respiration transiently on the basis of endogenous fuel substrates and phosphorylates only a small portion of the added ADP. State 2 is then obtained at a low respiratory activity limited by exhausted endogenous fuel substrate availability (**Table 3**). If addition of specific inhibitors of respiratory complexes, such as rotenone, does not cause a further decline of oxygen consumption, State 2 is equivalent to residual oxygen consumption (See below.). If inhibition is observed, undefined endogenous fuel substrates are a confounding factor of pathway control, contributing to the effect of subsequently externally added substrates and inhibitors. In contrast to the original protocol, an alternative sequence of titration steps is frequently applied, in which the alternative 'State 2' has an entirely different meaning, when this second state is induced by addition of fuel substrate without ADP (LEAK-state; in contrast to State 2 defined in **Table 2** as a ROX state), followed by addition of ADP.

651

652

653

654

655

656

657

658

659

660

661

662

663

664

State 3 is the state stimulated by addition of fuel substrates while the ADP concentration is still high (**Table 3**) and supports coupled energy transformation through oxidative phosphorylation. 'High ADP' is a concentration of ADP specifically selected to allow the measurement of State 3 to State 4 transitions of isolated mitochondria in a closed respirometric chamber. Repeated ADP titration re-establishes State 3 at 'high ADP'. Starting at oxygen concentrations near air-saturation (ca. 200 μ M O₂ at sea level and 37 °C), the total ADP concentration added must be low enough (typically 100 to 300 μ M) to allow phosphorylation to ATP at a coupled rate of oxygen consumption that does not lead to oxygen depletion during the transition to State 4. In contrast, kinetically-saturating ADP concentrations usually are an order of magnitude higher than 'high ADP', *e.g.* 2.5 mM in isolated mitochondria. The abbreviation State 3u is occasionally used in bioenergetics, to indicate the state of respiration after titration of an uncoupler, without sufficient emphasis on the fundamental difference between OXPHOS-capacity (*well-coupled* with an *endogenous* uncoupled component) and ET-capacity (*noncoupled*).

665

666

State 4 is a LEAK-state that is obtained only if the mitochondrial preparation is intact and well-coupled. Depletion of ADP by phosphorylation to ATP leads to a decline in the rate

667 of oxygen consumption in the transition from State 3 to State 4. Under these conditions, a
 668 maximum protonmotive force and high ATP/ADP ratio are maintained, and the P_{\gg}/O_2 ratio can
 669 be calculated. State 4 respiration, L_T (**Table 1**), reflects intrinsic proton leak and intrinsic ATP
 670 hydrolysis activity. Oxygen consumption in State 4 is an overestimation of LEAK-respiration
 671 if the contaminating ATP hydrolysis activity recycles some ATP to ADP, $J_{P\ll}$, which stimulates
 672 respiration coupled to phosphorylation, $J_{P\gg} > 0$. This can be tested by inhibition of the
 673 phosphorylation-pathway using oligomycin, ensuring that $J_{P\gg} = 0$ (State 4o). Alternatively,
 674 sequential ADP titrations re-establish State 3, followed by State 3 to State 4 transitions while
 675 sufficient oxygen is available. However, anoxia may be reached before exhaustion of ADP
 676 (State 5).

677 **State 5** is the state after exhaustion of oxygen in a closed respirometric chamber.
 678 Diffusion of oxygen from the surroundings into the aqueous solution may be a confounding
 679 factor preventing complete anoxia (Gnaiger 2001). Chance and Williams (1955) provide an
 680 alternative definition of State 5, which gives it the meaning of ROX: ‘State 5 may be obtained
 681 by antimycin A treatment or by anaerobiosis’.

682 In **Table 3**, only States 3 and 4 (and ‘State 2’ in the alternative protocol without ADP;
 683 not included in the table) are coupling control states, with the restriction that O_2 flux in State 3
 684 may be limited kinetically by non-saturating ADP concentrations (**Table 1**).
 685

686 3. The protonmotive force and proton flux

687 3.1. Electric and chemical partial forces versus electrical and chemical units

688 The protonmotive force across the mtIM (Mitchell 1961; Mitchell and Moyle 1967) was
 689 introduced most beautifully in the *Grey Book 1966* (Mitchell 2011),

$$690 \Delta p = \Delta \Psi + \Delta \mu_{H^+}/F \quad (\text{Eq. 1})$$

691 The protonmotive force, Δp , consists of two partial forces: (1) The electric part, $\Delta \Psi$, is the
 692 difference of charge (electric potential difference), is not specific for H^+ , and can, therefore, be
 693 measured by the distribution of other permeable cations between the positive and negative
 694 compartment (**Fig. 2**). (2) The chemical part contains the chemical potential difference in H^+ ,
 695 $\Delta \mu_{H^+}$, which is proportional to the pH difference, ΔpH (**Table 4**).
 696

697 **Table 4. Protonmotive force and flux matrix.** Columns: The protonmotive force is
 698 the sum of two *partial isomorphic forces*, $F_{el} + F_{H^+,d}$. Rows: Electrical and chemical
 699 formats (motive units, MU: C and mol, for e and n , respectively). The Faraday constant,
 700 F , converts protonmotive force and flux from format e to n . In contrast to force (state),
 701 the conjugated flux (rate) cannot be partitioned.
 702

State	Force		electric	+ chem.	Unit	Notes
Protonmotive force, e	Δp	=	$\Delta \Psi$	+ $\Delta \mu_{H^+}/F$	$J \cdot C^{-1}$	1e
Chemiosmotic potential, n	$\Delta \tilde{\mu}_{H^+}$	=	$\Delta \Psi \cdot F$	+ $\Delta \mu_{H^+}$	$J \cdot \text{mol}^{-1}$	1n
State	Isomorphic force		el	+ H^+,d	$J \cdot \text{MU}^{-1}$	
Electric charge, e	$F_{H^+/e}$	=	$F_{el/e}$	+ $F_{H^+,d/e}$	$J \cdot C^{-1}$	2e
Amount of substance, n	$F_{H^+/n}$	=	$F_{el/n}$	+ $F_{H^+,d/n}$	$J \cdot \text{mol}^{-1}$	2n
Rate	Isomorphic flux		e	or n	$\text{MU} \cdot \text{s}^{-1} \cdot \text{m}^{-3}$	
Electric charge, e	$J_{H^+/e}$		$J_{H^+/e}$		$C \cdot \text{s}^{-1} \cdot \text{m}^{-3}$	3e
Amount of substance, n	$J_{H^+/n}$			$J_{H^+/n}$	$\text{mol} \cdot \text{s}^{-1} \cdot \text{m}^{-3}$	3n

703
 704 1: The Faraday constant, F , is the product of elementary charge ($e = 1.602\,176\,634 \cdot 10^{-19}$ C) and the
 705 Avogadro (Loschmidt) constant ($N_A = 6.022\,140\,76 \cdot 10^{23}$ mol⁻¹), $F = e \cdot N_A = 96,485.33$ C·mol⁻¹ (Gibney
 706 2017). F is the conversion factor between electrical and chemical units. $\Delta \tilde{\mu}_{H^+}$ is the chemiosmotic
 707 potential difference. 1e and 1n are the classical representations of 2e and 2n.

- 708 2: F_{H^+} is the protonmotive force expressed in formats e [C] or n [mol]. $F_{el/e} \equiv \Delta\Psi$ is the partial
 709 protonmotive force (el) acting generally on charged motive molecules (*i.e.* ions that are permeable
 710 across the mtIM). In contrast, $F_{H^+,d/n} \equiv \Delta\mu_{H^+}$ is the partial protonmotive force specific for proton
 711 diffusion, H^+_d , irrespective of charge. The sign of the force is negative for exergonic transformations
 712 in which exergy is lost or dissipated, $F_{H^+,neg}$, and positive for endergonic transformations which
 713 conserve exergy in a coupled exergonic process, $F_{H^+,pos} = -F_{H^+,neg}$ (**Box 3**).
- 714 3: The sign of the flux, J_{H^+} , depends on the definition of the compartmental direction of the translocation.
 715 Flux in the outward direction into the positively (pos) charged compartment, $J_{H^+,pos}$, is positive when
 716 H^+_{pos} is added to the pos-compartment ($v_{H^+,pos} = 1$), and H^+_{neg} is removed stoichiometrically ($v_{H^+,neg}$
 717 $= -1$). Conversely, $J_{H^+,neg}$ is positive when H^+_{neg} is added to the negatively charged compartment
 718 ($v_{H^+,neg} = 1$) and H^+_{pos} is removed ($v_{H^+,pos} = -1$; **Fig. 2**). By definition, the product of flux and force is
 719 volume-specific power [$J \cdot s^{-1} \cdot m^{-3} = W \cdot m^{-3}$]: $P_{V,H^+} = J_{H^+,pos/e} \cdot F_{H^+,pos/e} = J_{H^+,pos/n} \cdot F_{H^+,pos/n}$.

721 **Faraday constant**, $F = e \cdot N_A$ [C/mol] (**Table 4**, note 1) enables the conversion between
 722 protonmotive force, $F_{H^+/e} \equiv \Delta p$ [J/C], expressed per *motive charge*, e [C], and protonmotive
 723 force, $F_{H^+/n} \equiv \Delta\tilde{\mu}_{H^+} = \Delta p \cdot F$ [J/mol], expressed per *motive amount of protons*, n [mol]. Proton
 724 charge, e , and amount of substance, n , are motive entities expressed in units C and mol,
 725 respectively. Taken together, F is the conversion factor for expressing protonmotive force and
 726 flux in motive units of e or n (Eq. 2; **Table 4**, Notes 1 and 2),

$$727 F_{H^+/n} = F_{H^+/e} \cdot (e \cdot N_A) \quad (\text{Eq. 2.1})$$

$$728 J_{H^+/n} = J_{H^+/e} / (e \cdot N_A) \quad (\text{Eq. 2.2})$$

729 In each format, the protonmotive force is expressed as the sum of two partial isomorphic
 730 forces. The complex symbols in Eq. 1 can be explained and visualized more explicitly by
 731 *partial isomorphic forces* as the components of the protonmotive force:

732 **Electric part of the protonmotive force:** (1) Isomorph e : $F_{el/e} \equiv \Delta\Psi$ is the electric part
 733 of the protonmotive force expressed in electrical units joule per coulomb, *i.e.* volt [$V = J/C$].
 734 $F_{el/e}$ is defined as partial Gibbs energy change per *motive elementary charge*, e [C], not specific
 735 for proton charge (**Table 4**, Note 2e). (2) Isomorph n : $F_{el/n} \equiv \Delta\Psi \cdot F$ is the electric force expressed
 736 in chemical units joule per mole [J/mol], defined as partial Gibbs energy change per *motive*
 737 *amount of charge*, n [mol], not specific for proton charge (**Table 4**, Note 2n).

738 **Chemical part of the protonmotive force:** (1) Isomorph n : $F_{H^+,d/n} \equiv \Delta\mu_{H^+}$ is the chemical
 739 part (diffusion, displacement of H^+) of the protonmotive force expressed in units joule per mole
 740 [J/mol]. $F_{H^+,d/n}$ is defined as partial Gibbs energy change per *motive amount of protons*, n [mol]
 741 (**Table 4**, Note 2n). (2) Isomorph e : $F_{H^+,d/e} \equiv \Delta\mu_{H^+}/F$ is the chemical force expressed in units
 742 joule per coulomb [$J/C = V$], defined as partial Gibbs energy change per *motive amount of*
 743 *protons expressed in units of electric charge*, e [C], but specific for proton charge (**Table 4**,
 744 Note 2e).

745 Protonmotive means that there is a potential for the movement of protons, and force is a
 746 measure of the potential for motion. Motion is relative and not absolute (Principle of Galilean
 747 Relativity); likewise there is no absolute potential, but isomorphic forces are potential
 748 differences (**Table 5**, Notes 5 and 6),

$$749 F_{el/n} = \Delta\psi \cdot zF = RT \cdot \Delta \ln c_{Bz} \quad (\text{Eq. 3.1})$$

$$750 F_{H^+,d/n} = \Delta\mu_{H^+} = RT \cdot \Delta \ln c_{H^+} \quad (\text{Eq. 3.2})$$

751 The isomorphism of the electric and chemical partial forces is most clearly illustrated when
 752 expressing all terms (Eq. 3) as dimensionless quantities (Eq. 4). For diffusion of protons into
 753 the matrix space (**Fig. 2**),

$$754 F_{el,neg/n} \cdot RT^{-1} = \ln(c_{Bz,pos}/c_{Bz,neg}) \quad (\text{Eq. 4.1})$$

$$755 F_{H^+,neg,d/n} \cdot RT^{-1} = \ln(c_{H^+,pos}/c_{H^+,neg}) \quad (\text{Eq. 4.2})$$

756
757
758
759
760

Table 5. Power, exergy, force, flux, and advancement.

Expression	Symbol	Definition	Unit	Notes
Power, volume-specific	$P_{V, \text{tr}}$	$P_{V, \text{tr}} = J_{\text{tr}} \cdot F_{\text{tr}} = d_{\text{tr}} G \cdot dt^{-1}$	$\text{W} \cdot \text{m}^{-3} = \text{J} \cdot \text{s}^{-1} \cdot \text{m}^{-3}$	1
Force, isomorphic	F_{tr}	$F_{\text{tr}} = \partial G / \partial \xi_{\text{tr}}^{-1}$	$\text{J} \cdot \text{MU}^{-1}$	2
Flux, isomorphic	J_{tr}	$J_{\text{tr}} = d_{\text{tr}} \xi_{\text{tr}} \cdot dt^{-1} \cdot V^{-1}$	$\text{MU} \cdot \text{s}^{-1} \cdot \text{m}^{-3}$	3
Advancement, n	$d_{\text{tr}} \xi_{\text{H}^+/n}$	$d_{\text{tr}} \xi_{\text{H}^+/n} = d_{\text{tr}} n_{\text{H}^+} \cdot \nu_{\text{H}^+}^{-1}$	$\text{MU} = \text{mol}$	$4n$
Advancement, e	$d_{\text{tr}} \xi_{\text{H}^+/e}$	$d_{\text{tr}} \xi_{\text{H}^+/e} = d_{\text{tr}} e_{\text{H}^+} \cdot \nu_{\text{H}^+}^{-1}$	$\text{MU} = \text{C}$	$4e$
Electric partial force, e	$F_{e/e}$	$F_{e/e} \equiv \Delta \Psi = RT / (zF) \cdot \Delta \ln a_{Bz}$	$\text{V} = \text{J} \cdot \text{C}^{-1}$	$5e$
Electric partial force, n	$F_{e/n}$	$F_{e/n} \equiv \Delta \Psi \cdot zF = RT \cdot \Delta \ln a_{Bz}$	$\text{kJ} \cdot \text{mol}^{-1}$	$5n$
	at $z = 1$	$= 96.5 \cdot \Delta \Psi$	$\text{kJ} \cdot \text{mol}^{-1}$	
Chemical partial force, e	$F_{\text{H}^+, d/e}$	$F_{\text{H}^+, d/e} \equiv \Delta \mu_{\text{H}^+} / F = -RT / F \cdot \ln(10) \cdot \Delta \text{pH}$	$\text{J} \cdot \text{C}^{-1}$	$6e$
	at 37°C	$= -0.061 \cdot \Delta \text{pH}$	$\text{J} \cdot \text{C}^{-1}$	
Chemical partial force, n	$F_{\text{H}^+, d/n}$	$F_{\text{H}^+, d/n} \equiv \Delta \mu_{\text{H}^+} = -RT \cdot \ln(10) \cdot \Delta \text{pH}$	$\text{J} \cdot \text{mol}^{-1}$	$6n$
	at 37°C	$= -5.9 \cdot \Delta \text{pH}$	$\text{kJ} \cdot \text{mol}^{-1}$	

763

764 1 to 4: A motive entity, expressed in a motive unit [MU] is a characteristic for any type of transformation,
765 tr. $\text{MU} = \text{mol}$ or C in the chemical or electrical format of proton translocation.

766 2: Isomorphic forces, F_{tr} , are related to the generalized forces, X_{tr} , of irreversible thermodynamics
767 as $F_{\text{tr}} = -X_{\text{tr}} \cdot T$, and the force of chemical reactions is the negative affinity, $F_{\text{r}} = -A$ (Prigogine 1967).
768 ∂G [J] is the partial Gibbs energy change in the advancement of transformation tr.

769 3: For $\text{MU} = \text{C}$, flow is electric current, I_{el} [$\text{A} = \text{C} \cdot \text{s}^{-1}$], vector flux is electric current density per area,
770 \mathbf{J}_{el} , and compartmental flux is electric current density per volume, I_{el} [$\text{A} \cdot \text{m}^{-3}$], all expressed in
771 electrical format.

772 $4n$: For a chemical reaction, the advancement of reaction r is $d_r \xi_B = d_r n_B \cdot \nu_B^{-1}$ [mol]. The stoichiometric
773 number is $\nu_B = -1$ or $\nu_B = 1$, depending on B being a product or substrate, respectively, in reaction
774 r involving one mole of B. The conjugated *intensive* molar quantity, $F_{B,r} = \partial G / \partial \xi_B$ [$\text{J} \cdot \text{mol}^{-1}$], is the
775 chemical force of reaction or *reaction-motive* force per stoichiometric amount of B. In reaction
776 kinetics, $d_r n_B$ is expressed as a volume-specific quantity, which is the partial contribution to the
777 total concentration change of B, $d_r c_B = d_r n_B / V$ and $dc_B = dn_B / V$, respectively. In open systems with
778 constant volume V , $dc_B = d_r c_B + d_e c_B$, where r indicates the *internal* reaction and e indicates the
779 *external* flux of B into the unit volume of the system. At steady state the concentration does not
780 change, $dc_B = 0$, when $d_r c_B$ is compensated for by the external flux of B, $d_r c_B = -d_e c_B$ (Gnaiger
781 1993b). Alternatively, $dc_B = 0$ when B is held constant by different coupled reactions in which B
782 acts as a substrate or a product.

783 $4e$: Scalar potential difference across the mitochondrial membrane. In a scalar electric transformation
784 (flux of charge, *i.e.* volume-specific current, from the matrix space to the intermembrane and
785 extramitochondrial space), the motive force is the difference of charge (**Box 2**). The endergonic
786 direction of translocation is defined in **Fig. 2** as $\text{H}^+_{\text{neg}} \rightarrow \text{H}^+_{\text{pos}}$.

787 $5e$: $F = 96.5$ ($\text{kJ} \cdot \text{mol}^{-1}$) / V . z_B is the charge number of ion B. a_B is the (relative) activity of ion B, which
788 in dilute solutions ($c < 0.1$ $\text{mol} \cdot \text{dm}^{-3}$) is approximately equal to c_B / c° , where c° is the standard
789 concentration of 1 $\text{mol} \cdot \text{dm}^{-3}$. $\Delta \ln a_B = \ln a_2 - \ln a_1 = \ln(a_2 / a_1)$, when ion B diffuses or is translocated
790 from compartment 1 to 2 (Eq. 4). Compartments 1 and 2 have to be defined in each case (**Fig.**
791 **2**). Note that ion selective electrodes (pH or TPP^+ electrodes) respond to $\ln a_B$. $\Delta \ln a_{\text{H}^+} = -$
792 $\ln(10) \cdot \Delta \text{pH}$.

- 793 6: $R = 8.31451 \text{ J}\cdot\text{mol}^{-1}\cdot\text{K}^{-1}$ is the gas constant. $RT = 2.479$ and $2.579 \text{ kJ}\cdot\text{mol}^{-1}$ at 298.15 and 310.15
 794 K (25 and 37 °C), respectively. See Eq. 3 and 4.
 795 6e: $RT/F\Delta\ln a_{\text{H}^+}$ yields force in the electrical format [$\text{J}\cdot\text{C}^{-1} = \text{V}$]. $RT/F = 2.479$ and 2.579 mV at 298.15
 796 and 310.15 K, respectively, and $\ln(10)\cdot RT/F = 59.16$ and 61.54 mV , respectively.
 797 6n: $RT\Delta\ln a_{\text{H}^+}$ yields force in the chemical format [$\text{J}\cdot\text{mol}^{-1}$]. $\ln(10)\cdot RT = 5.708$ and $5.938 \text{ kJ}\cdot\text{mol}^{-1}$ at
 798 298.15 and 310.15 K, respectively.
 799

800 An electric partial force of 0.2 V, expressed in the format of electric charge, $F_{\text{el, pos/e}}$ (**Table**
 801 **5**, Note 5e), can be expressed equivalently as $19 \text{ kJ}\cdot\text{mol}^{-1} \text{H}^+_{\text{pos}}$, in the format of amount, $F_{\text{el, pos/n}}$
 802 (Note 5n). For a ΔpH of 1 unit, the chemical partial force in the format of amount, $F_{\text{H}^+, \text{pos, d/n}}$,
 803 changes by $5.9 \text{ kJ}\cdot\text{mol}^{-1}$ (**Table 5**, Note 6n), and chemical force in the format of charge,
 804 $F_{\text{H}^+, \text{pos, d/e}}$, changes by 0.06 V (Note 6e). Considering a driving force of $-470 \text{ kJ}\cdot\text{mol}^{-1} \text{O}_2$ for
 805 oxidation, the thermodynamic limit of the $\text{H}^+_{\text{pos}}/\text{O}_2$ ratio is reached at a value of $470/19 = 24$,
 806 compared to a mechanistic stoichiometry of 20 (**Fig. 1**).
 807

808 3.2. Definitions

809 **Control and regulation:** The terms metabolic *control* and *regulation* are frequently used
 810 synonymously, but are distinguished in metabolic control analysis: ‘We could understand the
 811 regulation as the mechanism that occurs when a system maintains some variable constant over
 812 time, in spite of fluctuations in external conditions (homeostasis of the internal state). On the
 813 other hand, metabolic control is the power to change the state of the metabolism in response to
 814 an external signal’ (Fell 1997). Respiratory control may be induced by experimental control
 815 signals that *exert* an influence on: (1) ATP demand and ADP phosphorylation-rate; (2) fuel
 816 substrate composition, pathway competition; (3) available amounts of substrates and oxygen,
 817 *e.g.*, starvation and hypoxia; (3) the protonmotive force, redox states, flux-force relationships,
 818 coupling and efficiency; (4) Ca^{2+} and other ions including H^+ ; (5) inhibitors, *e.g.*, nitric oxide
 819 or intermediary metabolites, such as oxaloacetate; (6) signalling pathways and regulatory
 820 proteins, *e.g.* insulin resistance, transcription factor HIF-1 or inhibitory factor 1. *Mechanisms*
 821 of respiratory control and regulation include adjustments of: (1) enzyme activities by allosteric
 822 mechanisms and phosphorylation; (2) enzyme content, concentrations of cofactors and
 823 conserved moieties (such as adenylates, nicotinamide adenine dinucleotide [NAD^+/NADH],
 824 coenzyme Q, cytochrome *c*); (3) metabolic channeling by supercomplexes; and (4)
 825 mitochondrial density (enzyme concentrations and membrane area) and morphology (cristae
 826 folding, fission and fusion). (5) Mitochondria are targeted directly by hormones, thereby
 827 affecting their energy metabolism (Lee *et al.* 2013; Gerö and Szabo 2016; Price and Dai 2016;
 828 Moreno *et al.* 2017). Evolutionary or acquired differences in the genetic and epigenetic basis
 829 of mitochondrial function (or dysfunction) between subjects and gene therapy; age; gender,
 830 biological sex, and hormone concentrations; life style including exercise and nutrition; and
 831 environmental issues including thermal, atmospheric, toxicological and pharmacological
 832 factors, exert an influence on all control mechanisms listed above. For reviews, see Brown
 833 1992; Gnaiger 1993a, 2009; 2014; Paradies *et al.* 2014; Morrow *et al.* 2017.

834 **Respiratory control and response:** Lack of control by a metabolic pathway, *e.g.*
 835 phosphorylation-pathway, does mean that there will be no response to a variable activating it,
 836 *e.g.* [ADP]. However, the reverse is not true as the absence of a response to [ADP] does not
 837 exclude the phosphorylation-pathway from having some degree of control. The degree of
 838 control of a component of the OXPHOS-pathway on an output variable, such as oxygen flux,
 839 will in general be different from the degree of control on other outputs, such as phosphorylation-
 840 flux or proton leak flux (**Box 2**). As such, it is necessary to be specific as to which input and
 841 output are under consideration (Fell 1997). Therefore, the term respiratory control is elaborated
 842 in more detail in the following section.

843 **Respiratory coupling control:** Respiratory control refers to the ability of mitochondria
 844 to adjust oxygen consumption in response to external control signals by engaging various

845 mechanisms of control and regulation. Respiratory control is monitored in a mitochondrial
 846 preparation under conditions defined as respiratory states. When phosphorylation of ADP to
 847 ATP is stimulated or depressed, an increase or decrease is observed in electron flux linked to
 848 oxygen consumption in respiratory coupling states of intact mitochondria ('controlled states' in
 849 the classical terminology of bioenergetics). Alternatively, coupling of electron transfer with
 850 phosphorylation is disengaged by disruption of the integrity of the mtIM or by uncouplers,
 851 functioning like a clutch in a mechanical system. The corresponding coupling control state is
 852 characterized by high levels of oxygen consumption without control by phosphorylation
 853 ('uncontrolled state'). Energetic coupling is defined in **Box 4**. Loss of coupling lowers the
 854 efficiency by intrinsic uncoupling and decoupling, or pathological dyscoupling. Such
 855 generalized uncoupling is different from switching to mitochondrial pathways that involve
 856 fewer than three proton pumps ('coupling sites': Complexes CI, CIII and CIV), bypassing CI
 857 through multiple electron entries into the Q-junction (**Fig. 1**). A bypass of CIII and CIV is
 858 provided by alternative oxidases, which reduce oxygen without proton translocation.
 859 Reprogramming of mitochondrial pathways may be considered as a switch of gears (changing
 860 the stoichiometry) rather than uncoupling (loosening the stoichiometry).

861 **Pathway control states** are obtained in mitochondrial preparations by depletion of
 862 endogenous substrates and addition to the mitochondrial respiration medium of fuel substrates
 863 (CHNO) and specific inhibitors, activating selected mitochondrial pathways (**Fig. 1**). Coupling
 864 control states and pathway control states are complementary, since mitochondrial preparations
 865 depend on an exogenous supply of pathway-specific fuel substrates and oxygen (Gnaiger 2014).
 866

867 **Box 2: Metabolic fluxes and flows: vectorial and scalar**

868 In mitochondrial electron transfer (**Fig. 1**), vectorial transmembrane proton flux is coupled
 869 through the proton pumps CI, CIII and CIV to the catabolic flux of scalar reactions, collectively
 870 measured as oxygen flux. In **Fig. 2**, the scalar catabolic reaction, k , of oxygen consumption,
 871 $J_{O_2,k}$ [$\text{mol}\cdot\text{s}^{-1}\cdot\text{m}^{-3}$], is expressed as oxygen flux per volume, V [m^3], of the instrumental chamber
 872 (the system).

873 Fluxes are *vectors*, if they have *spatial* direction in addition to magnitude. A vector flux
 874 (surface-density of flow) is expressed per unit cross-sectional area, A [m^2], perpendicular to the
 875 direction of flux. If *flows*, I , are defined as extensive quantities of the *system*, as vector or scalar
 876 flow, \mathbf{I} or I [$\text{mol}\cdot\text{s}^{-1}$], respectively, then the corresponding vector and scalar *fluxes*, \mathbf{J} , are
 877 obtained as $\mathbf{J} = \mathbf{I}\cdot A^{-1}$ [$\text{mol}\cdot\text{s}^{-1}\cdot\text{m}^{-2}$] and $J = I\cdot V^{-1}$ [$\text{mol}\cdot\text{s}^{-1}\cdot\text{m}^{-3}$], respectively, expressing flux as an
 878 area-specific vector or volume-specific scalar quantity.

879 Vectorial transmembrane proton fluxes, $J_{H^+,pos}$ and $J_{H^+,neg}$, are analyzed in a heterogenous
 880 compartmental system as a quantity with *directional* but not *spatial* information. Translocation
 881 of protons across the mtIM has a defined direction, either from the negative compartment
 882 (matrix space; negative, neg-compartment) to the positive compartment (inter-membrane
 883 space; positive, pos-compartment) or *vice versa* (**Fig. 2**). The arrows defining the direction of
 884 the translocation between the two compartments may point upwards or downwards, right or
 885 left, without any implication that these are actual directions in space. The pos-compartment is
 886 neither above nor below the neg-compartment in a spatial sense, but can be visualized arbitrarily
 887 in a figure in the upper position (**Fig. 2**). In general, the *compartmental direction* of vectorial
 888 translocation from the neg-compartment to the pos-compartment is defined by assigning the
 889 initial and final state as *ergodynamic compartments*, $H^+_{neg} \rightarrow H^+_{pos}$ or $0 = -H^+_{neg} + H^+_{pos}$, related
 890 to work (erg = work) that must be performed to lift the proton from a lower to a higher
 891 electrochemical potential or from the lower to the higher ergodynamic compartment (Gnaiger
 892 1993b).

893 In direct analogy to *vectorial* translocation, the direction of a *scalar* chemical reaction, A
 894 $\rightarrow B$ or $0 = -A + B$, is defined by assigning substrates and products, A and B, as ergodynamic
 895 compartments. O_2 is defined as a substrate in respiratory O_2 consumption, which together with

896 the fuel substrates comprises the substrate compartment of the catabolic reaction (**Fig. 2**).
 897 Volume-specific scalar O_2 flux is coupled (**Box 4**) to vectorial translocation. In order to
 898 establish a quantitative relation between the coupled fluxes, both $J_{O_2,k}$ and $J_{H^+,pos}$ must be
 899 expressed in identical units, $[mol \cdot s^{-1} \cdot m^{-3}]$ or $[C \cdot s^{-1} \cdot m^{-3}]$, yielding the H^+_{pos}/O_2 ratio (**Fig. 1**). The
 900 *vectorial* proton flux in compartmental translocation has *compartmental direction*,
 901 distinguished from a *vector* flux with *spatial direction*. Likewise, the corresponding
 902 protonmotive force is defined as an electrochemical potential *difference* between two
 903 compartments, in contrast to a *gradient* across the membrane or a vector force with defined
 904 *spatial direction*.

905
 906 **The steady-state:** Mitochondria represent a thermodynamically open system functioning
 907 as a biochemical transformation system in non-equilibrium states. State variables (protonmotive
 908 force; redox states) and metabolic fluxes (*rates*) are measured in defined mitochondrial
 909 respiratory *states*. Strictly, steady states can be obtained only in open systems, in which changes
 910 due to *internal* transformations, *e.g.*, O_2 consumption, are instantaneously compensated for by
 911 *external* fluxes *e.g.*, O_2 supply, such that oxygen concentration does not change in the system
 912 (Gnaiger 1993b). Mitochondrial respiratory states monitored in closed systems satisfy the
 913 criteria of pseudo-steady states for limited periods of time, when changes in the system
 914 (concentrations of O_2 , fuel substrates, ADP, P_i , H^+) do not exert significant effects on metabolic
 915 fluxes (respiration, phosphorylation). Such pseudo-steady states require respiratory media with
 916 sufficient buffering capacity and kinetically-saturating concentrations of substrates to be
 917 maintained, and thus depend on the kinetics of the processes under investigation. Proton
 918 turnover, $J_{\infty H^+}$, and ATP turnover, $J_{\infty P}$, proceed in the steady-state at constant $F_{H^+,pos}$, when $J_{H^+\infty}$
 919 $= J_{H^+,pos} = J_{H^+,neg}$, and at constant $F_{P\gg}$, when $J_{P\infty} = J_{P\gg} = J_{P\ll}$ (**Fig. 2**).

921 3.3. Forces and fluxes in physics and thermodynamics

922 According to its definition in physics, a potential difference and as such the *protonmotive*
 923 *force*, Δp , is not a force *per se* (Cohen *et al.* 2008). The fundamental forces of physics are
 924 distinguished from *motive forces* of statistical and irreversible thermodynamics.
 925 Complementary to the attempt towards unification of fundamental forces defined in physics,
 926 the concepts of Nobel laureates Lars Onsager, Erwin Schrödinger, Ilya Prigogine and Peter
 927 Mitchell unite (even if expressed in apparently unrelated terms) the diversity of *generalized* or
 928 ‘isomorphic’ *flux-force* relationships, the product of which links to entropy production and the
 929 Second Law of thermodynamics (Schrödinger 1944; Prigogine 1967). A *motive force* is the
 930 derivative of potentially available or ‘free’ energy (exergy) per *motive entity* (**Box 3**). Perhaps
 931 the first account of a *motive force* in energy transformation can be traced back to the Peripatetic
 932 school around 300 BC in the context of moving a lever, up to Newton’s motive force
 933 proportional to the alteration of motion (Coopersmith 2010). As a generalization, isomorphic
 934 motive forces are considered as *entropic forces* in physics (Wang 2010).

936 **Box 3: Endergonic and exergonic transformations, exergy and dissipation**

937 A chemical reaction, or any transformation, is exergonic if the Gibbs energy change (exergy)
 938 of the reaction is negative at constant temperature and pressure. The sum of Gibbs energy
 939 changes of all internal transformations in a system can only be negative, *i.e.* exergy is
 940 irreversibly dissipated. Endergonic reactions are characterized by positive Gibbs energies of
 941 reaction and cannot proceed spontaneously in the forward direction as defined. For instance,
 942 the endergonic reaction $P\gg$ is coupled to exergonic catabolic reactions, such that the total Gibbs
 943 energy change is negative, *i.e.* exergy must be dissipated for the reaction to proceed (**Fig. 2**).

944 In contrast, energy cannot be lost or produced in any internal process, which is the key
 945 message of the First Law of thermodynamics. Thus mitochondria are the sites of energy
 946 transformation but not energy production. Open and closed systems can gain energy and exergy

947 only by external fluxes, *i.e.* uptake from the environment. Exergy is the potential to perform
 948 work. In the framework of flux-force relationships (**Box 4**), the *partial* derivative of Gibbs
 949 energy per advancement of a transformation is an isomorphic force, F_{tr} (**Table 5**, Note 2). In
 950 other words, force is equal to exergy per motive entity (in integral form, this definition takes
 951 care of non-isothermal processes). This formal generalization represents an appreciation of the
 952 conceptual beauty of Peter Mitchell's innovation of the protonmotive force against the
 953 background of the established paradigm of the electromotive force (emf) defined at the limit of
 954 zero current (Cohen *et al.* 2008).

955
 956 **Vectorial and scalar forces, and fluxes:** In chemical reactions and osmotic or diffusion
 957 processes occurring in a closed heterogeneous system, such as a chamber containing isolated
 958 mitochondria, scalar transformations occur without measured spatial direction but between
 959 separate compartments (displacement between the matrix and intermembrane space) or
 960 between energetically-separated chemical substances (reactions from substrates to products).
 961 Hence, the corresponding fluxes are not vectorial but scalar, and are expressed per volume and
 962 not per membrane area (**Box 2**). The corresponding motive forces are also scalar potential
 963 *differences* across the membrane (**Table 5**), without taking into account the *gradients* across
 964 the 6 nm thick mtIM (Rich 2003).

965 **Coupling:** In energetics (ergodynamics), coupling is defined as an energy transformation
 966 fuelled by an exergonic (downhill) input process driving the advancement of an endergonic
 967 (uphill) output process. The (negative) output/input power ratio is the efficiency of a coupled
 968 energy transformation (**Box 4**). At the limit of maximum efficiency of a completely coupled
 969 system, the (negative) input power equals the (positive) output power, such that the total power
 970 approaches zero at the maximum efficiency of 1, and the process becomes fully reversible
 971 without any dissipation of exergy, *i.e.* without entropy production.

973 **Box 4: Coupling, power and efficiency, at constant temperature and pressure**

974 Energetic coupling means that two processes of energy transformation are linked such that the
 975 input power, P_{in} , is the driving element of the output power, P_{out} , and the (negative) out/input
 976 power ratio is the efficiency. In general, power is work per unit time [$J \cdot s^{-1} = W$]. When
 977 describing a system with volume V without information on the internal structure, the output is
 978 defined as the *external work* (exergy) performed by the *total* system on its environment. Such
 979 a system may be open for any type of exchange, or closed and thus allowing only heat and work
 980 to be exchanged across the system boundaries. This is the classical black box approach of
 981 thermodynamics. In contrast, in a colourful compartmental analysis of *internal* energy
 982 transformations (**Fig. 2**), the system is structured and described by definition of ergodynamic
 983 compartments (with information on the heterogeneity of the system; **Box 2**) and analysis of
 984 separate parts, *i.e.* a sequence of *partial* energy transformations, *tr*. At constant temperature and
 985 pressure, power per unit volume, $P_{V,tr} = P_{tr}/V$ [$W \cdot m^{-3}$], is the product of a volume-specific flux,
 986 J_{tr} , and its conjugated force, F_{tr} , and is directly linked to entropy production, $d_i S/dt = \sum_{tr} P_{tr}/T$
 987 [$W \cdot K^{-1}$], as generalized by irreversible thermodynamics (Prigogine 1967; Gnaiger 1993a,b).
 988 Output power of proton translocation and catabolic input power are (**Fig. 2**),

989 Output: $P_{H^+,pos}/V = J_{H^+,pos} \cdot F_{H^+,pos}$

990 Input: $P_k/V = J_{O_2,k} \cdot F_{O_2,k}$

991 $F_{O_2,k}$ is the exergonic input force with a negative sign, and, $F_{H^+,pos}$, is the endergonic output
 992 force with a positive sign (**Box 3**). Ergodynamic efficiency is the ratio of output/input power,
 993 or the flux ratio times force ratio (Gnaiger 1993a,b),

994
$$\varepsilon = \frac{P_{H^+,pos}}{-P_k} = \frac{J_{H^+,pos}}{J_{O_2,k}} \cdot \frac{F_{H^+,pos}}{-F_{O_2,k}}$$

995 The concept of incomplete coupling relates exclusively to the first term, *i.e.* the flux ratio, or
 996 H^+_{pos}/O_2 ratio (**Fig. 1**). Likewise, respirometric definitions of the P_{\gg}/O_2 ratio and biochemical

997 coupling efficiency (Section 3.2) consider flux ratios. In a completely coupled process, the
 998 power efficiency, ε , depends entirely on the force ratio, ranging from zero efficiency at an
 999 output force of zero, to the limiting output force and maximum efficiency of 1.0, when the total
 1000 power of the coupled process, $P_t = P_k + P_{H^+,pos}$, equals zero, and any net flows are zero at
 1001 ergodynamic equilibrium of a coupled process. Thermodynamic equilibrium is defined as the
 1002 state when all potentials (all forces) are dissipated and equilibrate towards their minima of zero.
 1003 In a fully or completely coupled process, output and input fluxes are directly proportional in a
 1004 fixed ratio technically defined as a stoichiometric relationship (a gear ratio in a mechanical
 1005 system). Such maximal stoichiometric output/input flux ratios are considered in OXPHOS
 1006 analysis as the upper limits or mechanistic H^+_{pos}/O_2 and P_{\gg}/O_2 ratios (**Fig. 1**).

1007
 1008 **Coupled versus bound processes:** Since the chemiosmotic theory describes the
 1009 mechanisms of coupling in OXPHOS, it may be interesting to ask if the electrical and chemical
 1010 parts of proton translocation are coupled processes. This is not the case according to the
 1011 definition of coupling. If the coupling mechanism is disengaged, the output process becomes
 1012 independent of the input process, and both proceed in their downhill (exergonic) direction (**Fig.**
 1013 **2**). It is not possible to physically uncouple the electrical and chemical processes, which are
 1014 only *theoretically* partitioned as electrical and chemical components. The electrical and
 1015 chemical partial protonmotive *forces*, $F_{el,pos}$ and $F_{H^+,pos,d}$, can be measured separately. In
 1016 contrast, the corresponding proton *flux*, $J_{H^+,pos}$, is non-separable, *i.e.*, cannot be uncoupled. Then
 1017 these are not *coupled* processes, but are defined as *bound* processes. The electrical and chemical
 1018 parts are tightly bound partial forces, since the flux cannot be partitioned but expressed only in
 1019 either an electrical or chemical format, $J_{H^+/e}$ or $J_{H^+/n}$ (**Table 4**).

1020 4. Normalization: fluxes and flows

1021 The challenges of measuring mitochondrial respiratory flux are matched by those of
 1022 normalization, whereby O_2 consumption may be considered as the numerator and normalization
 1023 as the complementary denominator, which are tightly linked in reporting the measurements in
 1024 a format commensurate with the requirements of a database.

1025 4.1. Flux per chamber volume

1026
 1027 When the reactor volume does not change during the reaction, which is typical for liquid
 1028 phase reactions, the volume-specific *flux of a chemical reaction* r is the time derivative of the
 1029 advancement of the reaction per unit volume, $J_{V,B} = d_r \zeta_B / dt \cdot V^{-1}$ [(mol·s⁻¹)·L⁻¹]. The *rate of*
 1030 *concentration change* is dc_B/dt [(mol·L⁻¹)·s⁻¹], where concentration is $c_B = n_B/V$. It is helpful to
 1031 make the subtle distinction between [(mol·s⁻¹)·L⁻¹] and [(mol·L⁻¹)·s⁻¹] for the fundamentally
 1032 different quantities of volume-specific flux and rate of concentration change, which merge to a
 1033 single expression only in closed systems. In open systems, external fluxes (such as O_2 supply)
 1034 are distinguished from internal transformations (metabolic flux, O_2 consumption). In a closed
 1035 system, external flows of all substances are zero and O_2 consumption (internal flow), I_{O_2}
 1036 [pmol·s⁻¹], causes a decline of the amount of O_2 in the system, n_{O_2} [nmol]. Normalization of
 1037 these quantities for the volume of the system, V [L = dm³], yields volume-specific O_2 flux, J_{V,O_2}
 1038 = I_{O_2}/V [nmol·s⁻¹·L⁻¹], and O_2 concentration, $[O_2]$ or $c_{O_2} = n_{O_2}/V$ [μ mol·L⁻¹ = μ M = nmol·mL⁻¹].
 1039 Instrumental background O_2 flux is due to external flux into a non-ideal closed respirometer,
 1040 such that total volume-specific flux has to be corrected for instrumental background O_2 flux,
 1041 *i.e.* O_2 diffusion into or out of the instrumental chamber. J_{V,O_2} is relevant mainly for
 1042 methodological reasons and should be compared with the accuracy of instrumental resolution
 1043 of background-corrected flux, *e.g.* ± 1 nmol·s⁻¹·L⁻¹ (Gnaiger 2001). ‘Metabolic’ or catabolic
 1044 indicates O_2 flux, $J_{O_2,k}$, corrected for instrumental background O_2 flux and chemical background
 1045 O_2 flux due to autoxidation of chemical components added to the incubation medium.
 1046
 1047

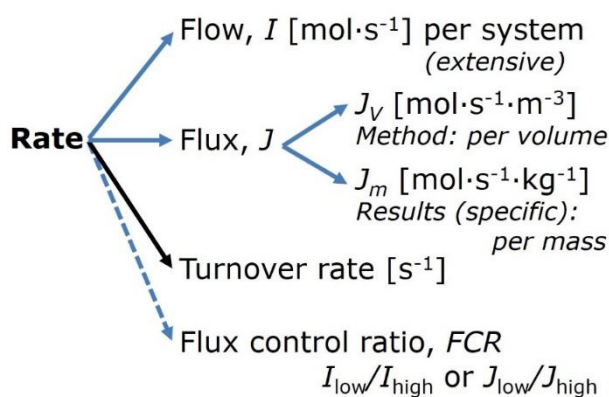
1048 4.2. System-specific and sample-specific normalization

1049 Application of common and generally defined units is required for direct transfer of
 1050 reported results into a database. The second [s] is the *SI* unit for the base quantity *time*. It is also
 1051 the standard time-unit used in solution chemical kinetics. **Table 6** lists some conversion factors
 1052 to obtain *SI* units. The term *rate* is not sufficiently defined to be useful for a database (**Fig. 7**).
 1053 The inconsistency of the meanings of rate becomes fully apparent when considering Galileo
 1054 Galilei's famous principle, that 'bodies of different weight all fall at the same rate (have a
 1055 constant acceleration)' (Coopersmith 2010).

1056 **Extensive quantities:** An extensive quantity increases proportionally with system size.
 1057 The magnitude of an extensive quantity is completely additive for non-interacting subsystems,
 1058 such as mass or flow expressed per defined system. The magnitude of these quantities depends
 1059 on the extent or size of the system (Cohen *et al.* 2008).

1060 **Size-specific quantities:** 'The adjective *specific* before the name of an extensive quantity
 1061 is often used to mean *divided by mass*' (Cohen *et al.* 2008). Mass-specific flux is flow divided
 1062 by mass of the system. A mass-specific quantity is independent of the extent of non-interacting
 1063 homogenous subsystems. Tissue-specific quantities are of fundamental interest in comparative
 1064 mitochondrial physiology, where *specific* refers to the *type* rather than *mass* of the tissue. The
 1065 term *specific*, therefore, must be further clarified, such that tissue mass-specific, *e.g.*, muscle
 1066 mass-specific quantities are defined.

1067 **Fig. 7. Different meanings of rate may lead**
 1068 **to confusion, if the normalization is not**
 1069 **sufficiently specified.** Results are frequently
 1070 expressed as mass-specific flux, J_m , per mg
 1071 protein, dry or wet weight (mass). Cell
 1072 volume, V_{cell} , or mitochondrial volume, V_{mt} ,
 1073 may be used for normalization (volume-
 1074 specific flux, $J_{V_{\text{cell}}}$ or $J_{V_{\text{mt}}}$), which then must
 1075 be clearly distinguished from flux, J_V ,
 1076 expressed for methodological reasons per
 1077 volume of the measurement system, or flow
 1078 per cell, I_X .



1081 **Molar quantities:** 'The adjective *molar* before the name of an extensive quantity
 1082 generally means *divided by amount of substance*' (Cohen *et al.* 2008). The notion that all molar
 1083 quantities then become *intensive* causes ambiguity in the meaning of *molar Gibbs energy*. It is
 1084 important to emphasize the fundamental difference between normalization for amount of
 1085 substance *in a system* or for amount of motive substance *in a transformation*. When the Gibbs
 1086 energy of a system, G [J], is divided by the amount of substance B in the system, n_B [mol], a
 1087 *size-specific* molar quantity is obtained, $G_B = G/n_B$ [J·mol⁻¹], which is not any force at all. In
 1088 contrast, when the partial Gibbs energy change, ∂G [J], is divided by the motive amount of
 1089 substance B in reaction r (advancement of reaction), $\partial_r \zeta_B$ [mol], the resulting intensive molar
 1090 quantity, $F_{B,r} = \partial G / \partial_r \zeta_B$ [J·mol⁻¹], is the chemical motive force of reaction r involving 1 mol B
 1091 (**Table 5**, Note 4).

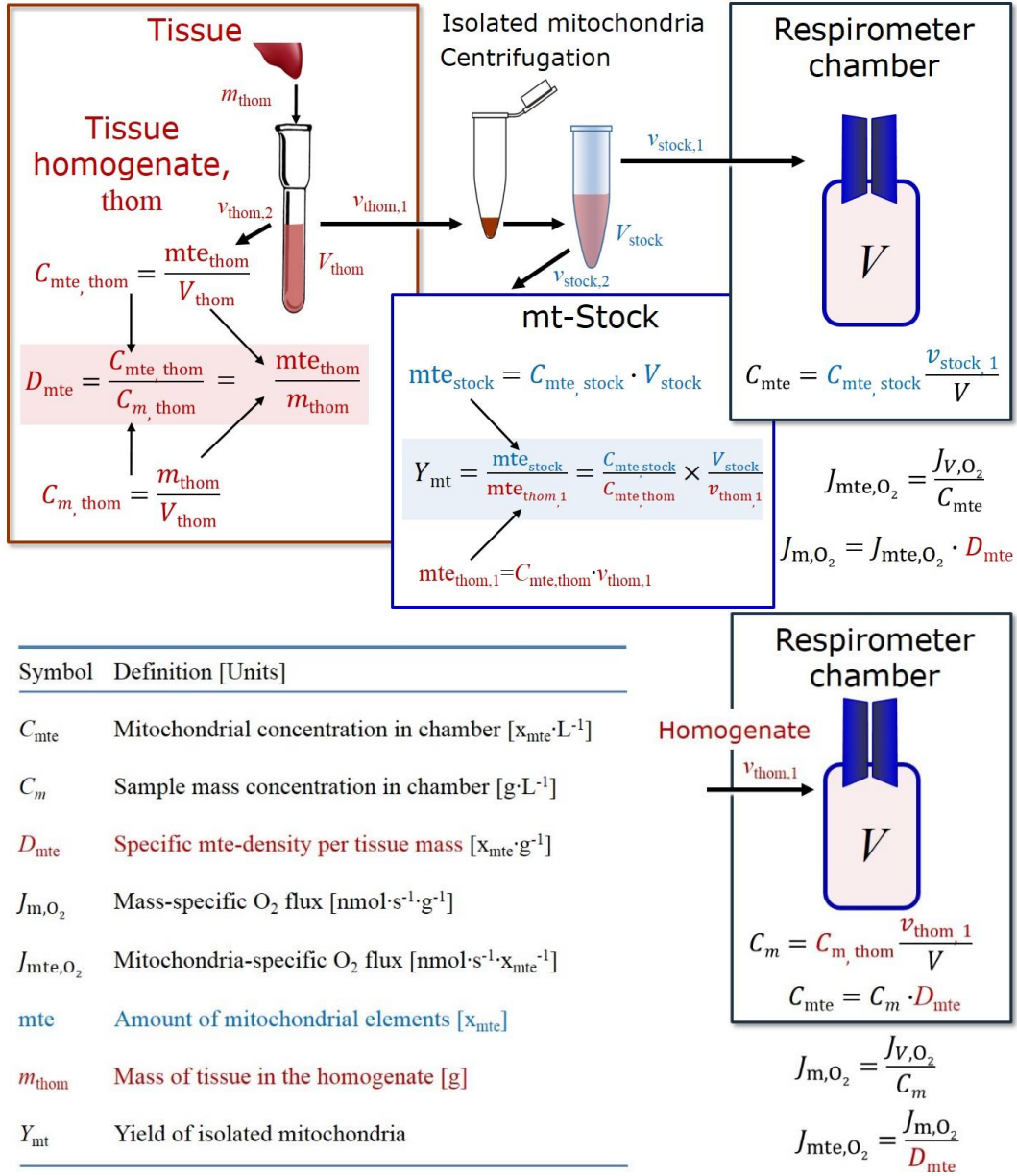
1092 **Flow per system, I :** In analogy to electrical terms, flow as an extensive quantity (I ; per
 1093 system) is distinguished from flux as a size-specific quantity (J ; per system size) (**Fig. 7**).
 1094 Electric current is flow, I_{el} [A = C·s⁻¹] per system (extensive quantity). When dividing this
 1095 extensive quantity by system size (membrane area), a size-specific quantity is obtained, which
 1096 is electric flux (electric current density), J_{el} [A·m⁻² = C·s⁻¹·m⁻²].

1097
 1098
 1099

Table 6. Sample concentrations and normalization of flux with SI/ base units.

Expression	Symbol	Definition	SI Unit	Notes
Sample				
Identity of sample	X	Cells, animals, patients		
Number of sample entities X	N_X	Number of cells, <i>etc.</i>	x	
Mass of sample X	m_X		kg	1
Mass of entity X	M_X	$M_X = m_X \cdot N_X^{-1}$	$\text{kg} \cdot \text{x}^{-1}$	1
Mitochondria				
Mitochondria	mt	$X = \text{mt}$		
Amount of mt-elements	mte	Quantity of mt-marker	x_{mte}	
Concentrations				
Sample number concentration	C_{NX}	$C_{NX} = N_X \cdot V^{-1}$	$\text{x} \cdot \text{m}^{-3}$	2
Sample mass concentration	C_{mX}	$C_{mX} = m_X \cdot V^{-1}$	$\text{kg} \cdot \text{m}^{-3}$	
Mitochondrial concentration	C_{mte}	$C_{\text{mte}} = \text{mte} \cdot V^{-1}$	$x_{\text{mte}} \cdot \text{m}^{-3}$	3
Specific mitochondrial density	D_{mte}	$D_{\text{mte}} = \text{mte} \cdot m_X^{-1}$	$x_{\text{mte}} \cdot \text{kg}^{-1}$	4
Mitochondrial content, mte per entity X	mte_X	$\text{mte}_X = \text{mte} \cdot N_X^{-1}$	$x_{\text{mte}} \cdot \text{x}^{-1}$	5
O₂ flow and flux				
Flow	I_{O_2}	Internal flow	$\text{mol} \cdot \text{s}^{-1}$	6
Volume-specific flux	J_{V,O_2}	$J_{V,\text{O}_2} = I_{\text{O}_2} \cdot V^{-1}$	$\text{mol} \cdot \text{s}^{-1} \cdot \text{m}^{-3}$	7
Flow per sample entity X	I_{X,O_2}	$I_{X,\text{O}_2} = J_{V,\text{O}_2} \cdot C_{NX}^{-1}$	$\text{mol} \cdot \text{s}^{-1} \cdot \text{x}^{-1}$	8
Mass-specific flux	J_{mX,O_2}	$J_{mX,\text{O}_2} = J_{V,\text{O}_2} \cdot C_{mX}^{-1}$	$\text{mol} \cdot \text{s}^{-1} \cdot \text{kg}^{-1}$	9
Mitochondria-specific flux	$J_{\text{mte},\text{O}_2}$	$J_{\text{mte},\text{O}_2} = J_{V,\text{O}_2} \cdot C_{\text{mte}}^{-1}$	$\text{mol} \cdot \text{s}^{-1} \cdot x_{\text{mte}}^{-1}$	10

- 1102
- 1103 1 The SI prefix k is used for the SI base unit of mass (kg = 1,000 g). In praxis, various SI prefixes are
- 1104 used for convenience, to make numbers easily readable, e.g. 1 mg tissue, cell or mitochondrial mass
- 1105 instead of 0.000001 kg.
- 1106 2 In case $X = \text{cells}$, the sample number concentration is $C_{N_{\text{cell}}} = N_{\text{cell}} \cdot V^{-1}$, and volume may be expressed
- 1107 in [$\text{dm}^3 = \text{L}$] or [$\text{cm}^3 = \text{mL}$]. See **Table 7** for different sample types.
- 1108 3 mt-concentration is an experimental variable, dependent on sample concentration: (1) $C_{\text{mte}} = \text{mte} \cdot V^{-1}$;
- 1109 (2) $C_{\text{mte}} = \text{mte}_X \cdot C_{NX}$; (3) $C_{\text{mte}} = C_{mX} \cdot D_{\text{mte}}$.
- 1110 4 If the amount of mitochondria, mte, is expressed as mitochondrial mass, then D_{mte} is the mass
- 1111 fraction of mitochondria in the sample. If mte is expressed as mitochondrial volume, V_{mt} , and the
- 1112 mass of sample, m_X , is replaced by volume of sample, V_X , then D_{mte} is the volume fraction of
- 1113 mitochondria in the sample.
- 1114 5 $\text{mte}_X = \text{mte} \cdot N_X^{-1} = C_{\text{mte}} \cdot C_{NX}^{-1}$.
- 1115 6 O₂ can be replaced by other chemicals B to study different reactions, e.g. ATP, H₂O₂, or
- 1116 compartmental translocations, e.g. Ca²⁺.
- 1117 7 I_{O_2} and V are defined per instrument chamber as a system of constant volume (and constant
- 1118 temperature), which may be closed or open. I_{O_2} is abbreviated for $I_{\text{O}_2,r}$, i.e. the metabolic or internal
- 1119 O₂ flow of the chemical reaction r in which O₂ is consumed, hence the negative stoichiometric
- 1120 number, $\nu_{\text{O}_2} = -1$. $I_{\text{O}_2,r} = d_r n_{\text{O}_2} / dt \cdot \nu_{\text{O}_2}^{-1}$. If r includes all chemical reactions in which O₂ participates, then
- 1121 $d_r n_{\text{O}_2} = dn_{\text{O}_2} - d_e n_{\text{O}_2}$, where dn_{O_2} is the change in the amount of O₂ in the instrument chamber and $d_e n_{\text{O}_2}$
- 1122 is the amount of O₂ added externally to the system. At steady state, by definition $dn_{\text{O}_2} = 0$, hence $d_r n_{\text{O}_2}$
- 1123 $= -d_e n_{\text{O}_2}$.
- 1124 8 J_{V,O_2} is an experimental variable, expressed per volume of the instrument chamber.
- 1125 9 I_{X,O_2} is a physiological variable, depending on the size of entity X .
- 1126 10 There are many ways to normalize for a mitochondrial marker, that are used in different experimental
- 1127 approaches: (1) $J_{\text{mte},\text{O}_2} = J_{V,\text{O}_2} \cdot C_{\text{mte}}^{-1}$; (2) $J_{\text{mte},\text{O}_2} = J_{V,\text{O}_2} \cdot C_{mX}^{-1} \cdot D_{\text{mte}}^{-1} = J_{mX,\text{O}_2} \cdot D_{\text{mte}}^{-1}$; (3) $J_{\text{mte},\text{O}_2} = J_{V,\text{O}_2} \cdot C_{NX}^{-1} \cdot \text{mte}_X^{-1}$
- 1128 $= I_{X,\text{O}_2} \cdot \text{mte}_X^{-1}$; (4) $J_{\text{mte},\text{O}_2} = I_{\text{O}_2} \cdot \text{mte}^{-1}$.
- 1129



1130

1131

1132

1133

1134

1135

1136

1137

1138

1139

1140

Fig. 8. Normalization of volume-specific flux of isolated mitochondria and tissue homogenate. **A:** Mitochondrial yield, Y_{mt} , in preparation of isolated mitochondria. $v_{thom,1}$ and $v_{stock,1}$ are the volumes transferred from the total volume, V_{thom} and V_{stock} , respectively. $mte_{thom,1}$ is the amount of mitochondrial elements in volume $v_{thom,1}$ used for isolation. **B:** In respirometry with homogenate, $v_{thom,1}$ is transferred directly into the respirometer chamber. See **Table 6** for further explanation of symbols.

Table 7. Some useful abbreviations of various sample types, X.

Identity of sample	X
Mitochondrial preparation	mtprep
Isolated mitochondria	imt
Tissue homogenate	thom
Permeabilized tissue	pti
Permeabilized fibre	pfi
Permeabilized cell	pce
Cell	ce
Organism	org

1141 **Size-specific flux, J :** Metabolic O_2 flow per tissue increases as tissue mass is increased.
 1142 Tissue mass-specific O_2 flux should be independent of the size of the tissue sample studied in
 1143 the instrument chamber, but volume-specific O_2 flux (per volume of the instrument chamber,
 1144 V) should increase in direct proportion to the amount of sample in the chamber. Accurate
 1145 definition of the experimental system is decisive: whether the experimental chamber is the
 1146 closed, open, isothermal or non-isothermal *system* with defined volume as part of the
 1147 measurement apparatus, in contrast to the experimental *sample* in the chamber (**Table 6**).
 1148 Volume-specific O_2 flux depends on mass-concentration of the sample in the chamber, but
 1149 should be independent of the chamber volume. There are practical limitations to increasing the
 1150 mass-concentration of the sample in the chamber, when one is concerned about crowding
 1151 effects and instrumental time resolution.

1152 **Sample concentration C_{mX} :** Normalization for sample concentration is required for
 1153 reporting respiratory data. Consider a tissue or cells as the sample, X , and the sample mass, m_X
 1154 [mg] from which a mitochondrial preparation is obtained. m_X is frequently measured as wet or
 1155 dry weight, W_w or W_d [mg], or as amount of tissue or cell protein, m_{Protein} . In the case of
 1156 permeabilized tissues, cells, and homogenates, the sample concentration, $C_{mX} = m_X/V$ [$\text{mg}\cdot\text{mL}^{-1}$
 1157 $= \text{g}\cdot\text{L}^{-1}$], is simply the mass of the subsample of tissue that is transferred into the instrument
 1158 chamber. Part of the mitochondria from the tissue is lost during preparation of isolated
 1159 mitochondria. The fraction of mitochondria obtained is expressed as mitochondrial yield (**Fig.**
 1160 **8**). At a high mitochondrial yield the sample of isolated mitochondria is more representative of
 1161 the total mitochondrial population than in preparations characterized by low mitochondrial
 1162 yield. Determination of the mitochondrial yield is based on measurement of the concentration
 1163 of a mitochondrial marker in the tissue homogenate, $C_{\text{mte,thom}}$, which simultaneously provides
 1164 information on the specific mitochondrial density in the sample (**Fig. 8**).

1165 Tissues can contain multiple cell populations which may have distinct mitochondrial
 1166 subtypes. Mitochondria undergo dynamic fission and fusion cycles, and can exist in multiple
 1167 stages and sizes which may be altered by a range of factors. The isolation of mitochondria (often
 1168 achieved through differential centrifugation) can therefore yield a subsample of the
 1169 mitochondrial types present in a tissue, dependent on isolation protocols utilized (*e.g.*
 1170 centrifugation speed). This possible artefact should be taken into account when planning
 1171 experiments using isolated mitochondria. The tendency for mitochondria of specific sizes to be
 1172 enriched at different centrifugation speeds also has the potential to allow the isolation of specific
 1173 mitochondrial subpopulations and therefore the analysis of mitochondria from multiple cell
 1174 lineages within a single tissue.

1175 **Mass-specific flux, J_{mX,O_2} :** Mass-specific flux is obtained by expressing respiration per
 1176 mass of sample, m_X [mg]. X is the type of sample, *e.g.*, tissue homogenate, permeabilized fibres
 1177 or cells. Volume-specific flux is divided by mass concentration of X , $J_{mX,O_2} = J_{V,O_2}/C_{mX}$; or flow
 1178 per cell is divided by mass per cell, $J_{m\text{cell},O_2} = I_{\text{cell},O_2}/M_{\text{cell}}$. If mass-specific O_2 flux is constant
 1179 and independent of sample size (expressed as mass), then there is no interaction between the
 1180 subsystems. A 1.5 mg and a 3.0 mg muscle sample respire at identical mass-specific flux.
 1181 Mass-specific O_2 flux, however, may change with the mass of a tissue sample, cells or isolated
 1182 mitochondria in the measuring chamber, in which case the nature of the interaction becomes an
 1183 issue. Optimization of cell density and arrangement is generally important and particularly in
 1184 experiments carried out in wells, considering the confluency of the cell monolayer or clumps
 1185 of cells (Salabei *et al.* 2014).

1186 **Number concentration, C_{NX} :** C_{NX} is the experimental *number concentration* of sample
 1187 in the case of cells or animals, *e.g.*, nematodes is $C_{NX} = N_X/V$ [$\text{x}\cdot\text{L}^{-1}$], where N_X is the number
 1188 of cells or organisms in the chamber (**Table 6**).

1189 **Flow per sample entity, I_{X,O_2} :** A special case of normalization is encountered in
 1190 respiratory studies with permeabilized (or intact) cells. If respiration is expressed per cell, the
 1191 O_2 flow per measurement system is replaced by the O_2 flow per cell, I_{cell,O_2} (**Table 6**). O_2 flow

1192 can be calculated from volume-specific O₂ flux, J_{V,O_2} [nmol·s⁻¹·L⁻¹] (per V of the measurement
 1193 chamber [L]), divided by the number concentration of cells, $C_{N_{ce}} = N_{ce}/V$ [cell·L⁻¹], where N_{ce}
 1194 is the number of cells in the chamber. Cellular O₂ flow can be compared between cells of
 1195 identical size. To take into account changes and differences in cell size, further normalization
 1196 is required to obtain cell size-specific or mitochondrial marker-specific O₂ flux (Renner *et al.*
 1197 2003).

1198 The complexity changes when the sample is a whole organism studied as an experimental
 1199 model. The well-established scaling law in respiratory physiology reveals a strong interaction
 1200 of O₂ consumption and individual body mass of an organism, since *basal* metabolic rate (flow)
 1201 does not increase linearly with body mass, whereas *maximum* mass-specific O₂ flux, \dot{V}_{O_2max} or
 1202 \dot{V}_{O_2peak} , is approximately constant across a large range of individual body mass (Weibel and
 1203 Hoppeler 2005), with individuals, breeds, and certain species deviating substantially from this
 1204 general relationship. \dot{V}_{O_2peak} of human endurance athletes is 60 to 80 mL O₂·min⁻¹·kg⁻¹ body
 1205 mass, converted to J_{m,O_2peak} of 45 to 60 nmol·s⁻¹·g⁻¹ (Gnaiger 2014; **Table 8**).
 1206

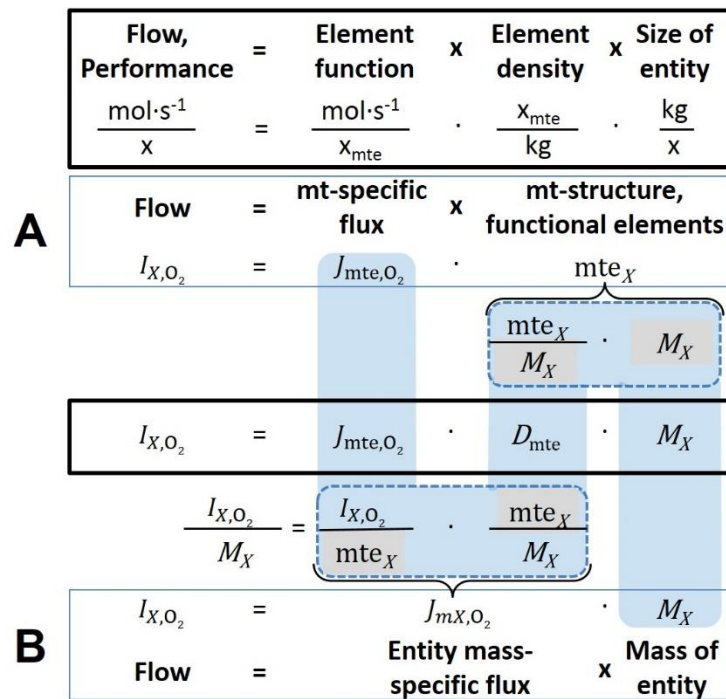
1207 4.3. Normalization for mitochondrial content

1208 Normalization is a problematic subject and it is essential to consider the question of the
 1209 study. If the study aims to compare tissue performance, such as the effects of a certain treatment
 1210 on a specific tissue, then normalization can be successful, using tissue mass or protein content,
 1211 for example. If the aim, however, is to find differences of mitochondrial function independent
 1212 of mitochondrial density (**Table 6**), then normalization to a mitochondrial marker is imperative
 1213 (**Fig. 9**). However, one cannot assume that quantitative changes in various markers such as
 1214 mitochondrial proteins necessarily occur in parallel with one another. It is important to first
 1215 establish that the marker chosen is not selectively altered by the performed treatment. In
 1216 conclusion, the normalization must reflect the question under investigation to reach a satisfying
 1217 answer. On the other hand, the goal of comparing results across projects and institutions
 1218 requires some standardization on normalization for entry into a databank.

1219 **Mitochondrial concentration, C_{mte} , and mitochondrial markers:** It is important that
 1220 mitochondrial concentration in the tissue and the measurement chamber be quantified, as a
 1221 physiological output and result of mitochondrial biogenesis and degradation, and as a quantity
 1222 for normalization in functional analyses. Mitochondrial organelles comprise a dynamic cellular
 1223 reticulum in various states of fusion and fission. Hence the definition of an "amount" of
 1224 mitochondria is often misconceived: mitochondria cannot be counted as a number of occurring
 1225 elements. Therefore, quantification of the "amount" of mitochondria depends on measurement
 1226 of chosen mitochondrial markers. 'Mitochondria are the structural and functional elemental
 1227 units of cell respiration' (Gnaiger 2014). The quantity of a mitochondrial marker can be
 1228 considered to reflect the amount of *elemental mitochondrial units* or *mitochondrial elements*,
 1229 *mte*. However, since mitochondrial quality changes under certain stimuli, particularly in
 1230 mitochondrial dysfunction and after exercise training (Pesta *et al.* 2011; Campos *et al.* 2017),
 1231 some markers can vary while other markers are unchanged: (1) Mitochondrial volume and
 1232 membrane area are structural markers, whereas mitochondrial protein mass is frequently used
 1233 as a marker for isolated mitochondria. (2) Molecular and enzymatic mitochondrial markers
 1234 (amounts or activities) can be selected as matrix markers, *e.g.*, citrate synthase activity, mtDNA;
 1235 mtIM-markers, *e.g.*, cytochrome *c* oxidase activity, *aa3* content, cardiolipin, or mtOM-markers,
 1236 *e.g.*, TOM20. (3) Extending the measurement of mitochondrial marker enzyme activity to
 1237 mitochondrial pathway capacity, measured as ET- or OXPHOS-capacity, can be considered as
 1238 an integrative functional mitochondrial marker.

1239 Depending on the type of mitochondrial marker, the mitochondrial elements, *mte*, are
 1240 expressed in marker-specific units. Although concentration and density are used synonymously
 1241 in physical chemistry, it is recommended to distinguish *experimental mitochondrial*
 1242 *concentration*, $C_{mte} = mte/V$ and *physiological mitochondrial density*, $D_{mte} = mte/m_x$. Then

1243 mitochondrial density is the amount of mitochondrial elements per mass of tissue (**Fig. 9**). The
 1244 former is mitochondrial density multiplied by sample mass concentration, $C_{\text{mte}} = D_{\text{mte}} \cdot C_{mX}$, or
 1245 mitochondrial content multiplied by sample number concentration, $C_{\text{mte}} = \text{mte}_X \cdot C_{NX}$ (**Table 6**).
 1246



1247
 1248 **Fig. 9. Structure-function analysis of performance of an organism, organ or tissue, or a**
 1249 **cell (sample entity X). O₂ flow, I_{X,O_2} , is the product of performance per functional element**
 1250 **(element function, mitochondria-specific flux), element density (mitochondrial density,**
 1251 **D_{mte}), and size of entity X (mass M_X). (A) Structured analysis: performance is the product of**
 1252 **mitochondrial function (mt-specific flux) and structure (functional elements; D_{mte} times mass**
 1253 **of X). (B) Unstructured analysis: performance is the product of entity mass-specific flux, J_{mX,O_2}**
 1254 **$= I_{X,O_2}/M_X = I_{O_2}/m_X$ [mol·s⁻¹·kg⁻¹] and size of entity, expressed as mass of X; $M_X = m_X \cdot N_X^{-1}$**
 1255 **[kg·X⁻¹]. See Table 6 for further explanation of quantities and units. Modified from Gnaiger**
 1256 **(2014).**
 1257

1258 **Mitochondria-specific flux, J_{mte,O_2} :** Volume-specific metabolic O₂ flux depends on: (1)
 1259 the sample concentration in the volume of the instrument chamber, C_{mX} , or C_{NX} ; (2) the
 1260 mitochondrial density in the sample, $D_{\text{mte}} = \text{mte}/m_X$ or $\text{mte}_X = \text{mte}/N_X$; and (3) the specific
 1261 mitochondrial activity or performance per elemental mitochondrial unit, $J_{\text{mte},O_2} = J_{V,O_2}/C_{\text{mte}}$
 1262 (**Table 6**). Obviously, the numerical results for J_{mte,O_2} vary according to the type of
 1263 mitochondrial marker chosen for measurement of mte and $C_{\text{mte}} = \text{mte}/V$.
 1264

1265 4.4. Evaluation of mitochondrial markers

1266 Different methods are implicated in quantification of mitochondrial markers and have
 1267 different strengths. Some problems are common for all mitochondrial markers, mte: (1)
 1268 Accuracy of measurement is crucial, since even a highly accurate and reproducible
 1269 measurement of O₂ flux results in an inaccurate and noisy expression normalized for a biased
 1270 and noisy measurement of a mitochondrial marker. This problem is acute in mitochondrial
 1271 respiration because the denominators used (the mitochondrial markers) are often very small
 1272 moieties whose accurate and precise determination is difficult. This problem can be avoided
 1273 when O₂ fluxes measured in substrate-uncoupler-inhibitor titration protocols are normalized for
 1274 flux in a defined respiratory reference state, which is used as an internal marker and yields flux
 1275 control ratios, FCRs (**Fig. 7**). FCRs are independent of any externally measured markers and,

1276 therefore, are statistically very robust, considering the limitations of ratios in general (Jasienski
 1277 and Bazzaz 1999). *FCRs* indicate qualitative changes of mitochondrial respiratory control, with
 1278 highest quantitative resolution, separating the effect of mitochondrial density or concentration
 1279 on J_{mX,O_2} and I_{X,O_2} from that of function per elemental mitochondrial marker, J_{mte,O_2} (Pesta *et al.*
 1280 2011; Gnaiger 2014). (2) If mitochondrial quality does not change and only the amount of
 1281 mitochondria varies as a determinant of mass-specific flux, any marker is equally qualified in
 1282 principle; then in practice selection of the optimum marker depends only on the accuracy and
 1283 precision of measurement of the mitochondrial marker. (3) If mitochondrial flux control ratios
 1284 change, then there may not be any best mitochondrial marker. In general, measurement of
 1285 multiple mitochondrial markers enables a comparison and evaluation of normalization for a
 1286 variety of mitochondrial markers. Particularly during postnatal development, the activity of
 1287 marker enzymes, such as cytochrome *c* oxidase and citrate synthase, follows different time
 1288 courses (Drahota *et al.* 2004). Evaluation of mitochondrial markers in healthy controls is
 1289 insufficient for providing guidelines for application in the diagnosis of pathological states and
 1290 specific treatments.

1291 In line with the concept of the respiratory control ratio (Chance and Williams 1955a), the
 1292 most readily used normalization is that of flux control ratios and flux control factors (Gnaiger
 1293 2014). Selection of the state of maximum flux in a protocol as the reference state has the
 1294 advantages of: (1) internal normalization; (2) statistical linearization of the response in the range
 1295 of 0 to 1; and (3) consideration of maximum flux for integrating a very large number of
 1296 elemental steps in the OXPHOS- or ET-pathways. This reduces the risk of selecting a functional
 1297 marker that is specifically altered by the treatment or pathodology, yet increases the chance that
 1298 the highly integrative pathway is disproportionately affected, *e.g.* the OXPHOS- rather than
 1299 ET-pathway in case of an enzymatic defect in the phosphorylation-pathway. In this case,
 1300 additional information can be obtained by reporting flux control ratios based on a reference
 1301 state which indicates stable tissue-mass specific flux. Stereological determination of
 1302 mitochondrial content via two-dimensional transmission electron microscopy can have
 1303 limitations due to the dynamics of mitochondrial size (Meinild Lundby *et al.* 2017). Accurate
 1304 determination of three-dimensional volume by two-dimensional microscopy can be both time
 1305 consuming and statistically challenging (Larsen *et al.* 2012). Using mitochondrial marker
 1306 enzymes (citrate synthase activity, Complex I–IV amount or activity) for normalization of flux
 1307 is limited in part by the same factors that apply to the use of flux control ratios. Strong
 1308 correlations between various mitochondrial markers and citrate synthase activity (Reichmann
 1309 *et al.* 1985; Boushel *et al.* 2007; Mogensen *et al.* 2007) are expected in a specific tissue of
 1310 healthy subjects and in disease states not specifically targeting citrate synthase. Citrate synthase
 1311 activity is acutely modifiable by exercise (Tonkonogi *et al.* 1997; Leek *et al.* 2001). Evaluation
 1312 of mitochondrial markers related to a selected age and sex cohort cannot be extrapolated to
 1313 provide recommendations for normalization in respirometric diagnosis of disease, in different
 1314 states of development and ageing, different cell types, tissues, and species. mtDNA normalised
 1315 to nDNA via qPCR is correlated to functional mitochondrial markers including OXPHOS- and
 1316 ET-capacity in some cases (Puntschart *et al.* 1995; Wang *et al.* 1999; Menshikova *et al.* 2006;
 1317 Boushel *et al.* 2007), but lack of such correlations have been reported (Menshikova *et al.* 2005;
 1318 Schultz and Wiesner 2000; Pesta *et al.* 2011). Several studies indicate a strong correlation
 1319 between cardiolipin content and increase in mitochondrial functionality with exercise
 1320 (Menshikova *et al.* 2005; Menshikova *et al.* 2007; Larsen *et al.* 2012; Faber *et al.* 2014), but its
 1321 use as a general mitochondrial biomarker in disease remains questionable.

1322 1323 4.5. Conversion: units and normalization

1324 Many different units have been used to report the rate of oxygen consumption, OCR
 1325 (**Table 8**). *SI* base units provide the common reference for introducing the theoretical principles
 1326 (**Fig. 7**), and are used with appropriately chosen *SI* prefixes to express numerical data in the

1327 most practical format, with an effort towards unification within specific areas of application
 1328 (**Table 9**). For studies of cells, we recommend that respiration be expressed, as far as possible,
 1329 as: (1) O₂ flux normalized for a mitochondrial marker, for separation of the effects of
 1330 mitochondrial quality and content on cell respiration (this includes *FCRs* as a normalization for
 1331 a functional mitochondrial marker); (2) O₂ flux in units of cell volume or mass, for comparison
 1332 of respiration of cells with different cell size (Renner *et al.* 2003) and with studies on tissue
 1333 preparations, and (3) O₂ flow in units of attomole (10⁻¹⁸ mol) of O₂ consumed in a second by
 1334 each cell [amol·s⁻¹·cell⁻¹], numerically equivalent to [pmol·s⁻¹·10⁻⁶ cells]. This convention
 1335 allows information to be easily used when designing experiments in which oxygen consumption
 1336 must be considered. For example, to estimate the volume-specific O₂ flux in an instrument
 1337 chamber that would be expected at a particular cell number concentration, one simply needs to
 1338 multiply the flow per cell by the number of cells per volume of interest. This provides the
 1339 amount of O₂ [mol] consumed per time [s⁻¹] per unit volume [L⁻¹]. At an O₂ flow of 100
 1340 amol·s⁻¹·cell⁻¹ and a cell density of 10⁹ cells·L⁻¹ (10⁶ cells·mL⁻¹), the volume-specific O₂ flux is
 1341 100 nmol·s⁻¹·L⁻¹ (100 pmol·s⁻¹·mL⁻¹).

1342 Although volume is expressed as m³ using the *SI* base unit, the litre [dm³] is the basic unit
 1343 of volume for concentration and is used for most solution chemical kinetics. If one multiplies
 1344 $I_{\text{cell},\text{O}_2}$ by C_{Ncell} , then the result will not only be the amount of O₂ [mol] consumed per time [s⁻¹]
 1345 in one litre [L⁻¹], but also the change in the concentration of oxygen per second (for any volume
 1346 of an ideally closed system). This is ideal for kinetic modeling as it blends with chemical rate
 1347 equations where concentrations are typically expressed in mol·L⁻¹ (Wagner *et al.* 2011). In
 1348 studies of multinuclear cells, such as differentiated skeletal muscle cells, it is easy to determine
 1349 the number of nuclei but not the total number of cells. A generalized concept, therefore, is
 1350 obtained by substituting cells by nuclei as the sample entity. This does not hold, however, for
 1351 enucleated platelets.
 1352

1353 4.5. Conversion: oxygen, proton and ATP flux

1354 $J_{\text{O}_2,\text{k}}$ is coupled in mitochondrial steady states to proton cycling, $J_{\text{H}^+\infty} = J_{\text{H}^+,\text{pos}} = J_{\text{H}^+,\text{neg}}$
 1355 (**Fig. 2**). $J_{\text{H}^+,\text{pos}/\text{n}}$ and $J_{\text{H}^+,\text{neg}/\text{n}}$ [nmol·s⁻¹·L⁻¹] are converted into electrical units, $J_{\text{H}^+,\text{pos}/\text{e}}$ [mC·s⁻¹·L⁻¹
 1356 = mA·L⁻¹] = $J_{\text{H}^+,\text{pos}/\text{n}}$ [nmol·s⁻¹·L⁻¹]· F [C·mol⁻¹]·10⁻⁶ (**Table 4**). At a $J_{\text{H}^+,\text{pos}}/J_{\text{O}_2,\text{k}}$ ratio or $\text{H}^+_{\text{pos}}/\text{O}_2$
 1357 of 20 ($\text{H}^+_{\text{pos}}/\text{O} = 10$), a volume-specific O₂ flux of 100 nmol·s⁻¹·L⁻¹ would correspond to a proton
 1358 flux of 2,000 nmol $\text{H}^+_{\text{pos}}\cdot\text{s}^{-1}\cdot\text{L}^{-1}$ or volume-specific current of 193 mA·L⁻¹.

$$1359 J_{V,\text{H}^+,\text{pos}/\text{e}} [\text{mA}\cdot\text{L}^{-1}] = J_{V,\text{H}^+,\text{pos}/\text{n}} \cdot F \cdot 10^{-6} [\text{nmol}\cdot\text{s}^{-1}\cdot\text{L}^{-1}\cdot\text{mC}\cdot\text{nmol}^{-1}] \quad (\text{Eq. 5.1})$$

$$1360 J_{V,\text{H}^+,\text{pos}/\text{e}} [\text{mA}\cdot\text{L}^{-1}] = J_{V,\text{O}_2} \cdot (\text{H}^+_{\text{pos}}/\text{O}_2) \cdot F \cdot 10^{-6} [\text{mC}\cdot\text{s}^{-1}\cdot\text{L}^{-1} = \text{mA}\cdot\text{L}^{-1}] \quad (\text{Eq. 5.2})$$

1361 ET-capacity in various human cell types including HEK 293, primary HUVEC and fibroblasts
 1362 ranges from 50 to 180 amol·s⁻¹·cell⁻¹, measured in intact cells in the noncoupled state (see
 1363 Gnaiger 2014). At 100 amol·s⁻¹·cell⁻¹ corrected for *Rox* (corresponding to a catabolic power of
 1364 -48 pW·cell⁻¹), the current across the mt-membranes, I_e , approximates 193 pA·cell⁻¹ or 0.2 nA
 1365 per cell. See Rich (2003) for an extension of quantitative bioenergetics from the molecular to
 1366 the human scale, with a transmembrane proton flux equivalent to 520 A in an adult at a catabolic
 1367 power of -110 W. Modelling approaches illustrate the link between protonmotive force and
 1368 currents (Willis *et al.* 2016). For NADH- and succinate-linked respiration, the mechanistic
 1369 $\text{P}\gg/\text{O}_2$ ratio (referring to the full 4 electron reduction of O₂) is calculated at 20/3.7 = 5.4 and
 1370 12/3.7 = 3.3, respectively (Eq. 6). The classical $\text{P}\gg/\text{O}$ ratios (referring to the 2 electron reduction
 1371 of 0.5 O₂) are 2.7 and 1.6 (Watt *et al.* 2010), in direct agreement with the measured $\text{P}\gg/\text{O}$ ratio
 1372 for succinate of 1.58 ± 0.02 (Gnaiger *et al.* 2000; for detailed reviews see Wikström and
 1373 Hummer 2012; Sazanov 2015),

$$1374 \text{P}\gg/\text{O}_2 = (\text{H}^+_{\text{pos}}/\text{O}_2)/(\text{H}^+_{\text{neg}}/\text{P}\gg) \quad (\text{Eq. 6})$$

1375 In summary (**Fig. 1**),

$$1376 J_{V,\text{P}\gg} [\text{nmol}\cdot\text{s}^{-1}\cdot\text{L}^{-1}] = J_{V,\text{O}_2} \cdot (\text{H}^+_{\text{pos}}/\text{O}_2)/(\text{H}^+_{\text{neg}}/\text{P}\gg) \quad (\text{Eq. 7.1})$$

$$1377 J_{V,\text{P}\gg} [\text{nmol}\cdot\text{s}^{-1}\cdot\text{L}^{-1}] = J_{V,\text{O}_2} \cdot (\text{P}\gg/\text{O}_2) \quad (\text{Eq. 7.2})$$

1378
1379
1380
1381**Table 8. Conversion of various units used in respirometry and ergometry.** e is the number of electrons or reducing equivalents. z_B is the charge number of entity B.

1 Unit	x	Multiplication factor	SI-Unit	Note
ng.atom O \cdot s $^{-1}$	(2 e)	0.5	nmol O $_2$ \cdot s $^{-1}$	
ng.atom O \cdot min $^{-1}$	(2 e)	8.33	pmol O $_2$ \cdot s $^{-1}$	
natom O \cdot min $^{-1}$	(2 e)	8.33	pmol O $_2$ \cdot s $^{-1}$	
nmol O $_2$ \cdot min $^{-1}$	(4 e)	16.67	pmol O $_2$ \cdot s $^{-1}$	
nmol O $_2$ \cdot h $^{-1}$	(4 e)	0.2778	pmol O $_2$ \cdot s $^{-1}$	
mL O $_2$ \cdot min $^{-1}$ at STPD ^a		0.744	μ mol O $_2$ \cdot s $^{-1}$	1
W = J/s at -470 kJ/mol O $_2$		-2.128	μ mol O $_2$ \cdot s $^{-1}$	
mA = mC \cdot s $^{-1}$	($z_{H^+} = 1$)	10.36	nmol H $^+$ \cdot s $^{-1}$	2
mA = mC \cdot s $^{-1}$	($z_{O_2} = 4$)	2.59	nmol O $_2$ \cdot s $^{-1}$	2
nmol H $^+$ \cdot s $^{-1}$	($z_{H^+} = 1$)	0.09649	mA	3
nmol O $_2$ \cdot s $^{-1}$	($z_{O_2} = 4$)	0.38594	mA	3

1382
1383
1384
1385
1386
1387
1388
1389
1390

- 1 At standard temperature and pressure dry (STPD: 0 °C = 273.15 K and 1 atm = 101.325 kPa = 760 mmHg), the molar volume of an ideal gas, V_m , and V_{m,O_2} is 22.414 and 22.392 L \cdot mol $^{-1}$ respectively. Rounded to three decimal places, both values yield the conversion factor of 0.744. For comparison at NTPD (20 °C), V_{m,O_2} is 24.038 L \cdot mol $^{-1}$. Note that the SI standard pressure is 100 kPa.
- 2 The multiplication factor is $10^6/(z_B \cdot F)$.
- 3 The multiplication factor is $z_B \cdot F/10^6$.

Table 9. Conversion of units with preservation of numerical values.

Name	Frequently used unit	Equivalent unit	Note
Volume-specific flux, J_{V,O_2}	pmol \cdot s $^{-1}$ \cdot mL $^{-1}$	nmol \cdot s $^{-1}$ \cdot L $^{-1}$	1
	mmol \cdot s $^{-1}$ \cdot L $^{-1}$	mol \cdot s $^{-1}$ \cdot m 3	
Cell-specific flow, I_{O_2}	pmol \cdot s $^{-1}$ \cdot 10 $^{-6}$ cells	amol \cdot s $^{-1}$ \cdot cell $^{-1}$	2
	pmol \cdot s $^{-1}$ \cdot 10 $^{-9}$ cells	zmol \cdot s $^{-1}$ \cdot cell $^{-1}$	3
Cell number concentration, C_{Nce}	10 6 cells \cdot mL $^{-1}$	10 9 cells \cdot L $^{-1}$	
Mitochondrial protein concentration, C_{mte}	0.1 mg \cdot mL $^{-1}$	0.1 g \cdot L $^{-1}$	
Mass-specific flux, J_{m,O_2}	pmol \cdot s $^{-1}$ \cdot mg $^{-1}$	nmol \cdot s $^{-1}$ \cdot g $^{-1}$	4
Catabolic power, $P_{O_2,k}$	μ W \cdot 10 $^{-6}$ cells	pW \cdot cell $^{-1}$	1
Volume	1,000 L	m 3 (1,000 kg)	
	L	dm 3 (kg)	
	mL	cm 3 (g)	
	μ L	mm 3 (mg)	
	fL	μ m 3 (pg)	5
Amount of substance concentration	M = mol \cdot L $^{-1}$	mol \cdot dm $^{-3}$	

1391
1392
1393
1394
1395

- 1 pmol: picomole = 10 $^{-12}$ mol
- 2 amol: attomole = 10 $^{-18}$ mol
- 3 zmol: zeptomole = 10 $^{-21}$ mol
- 4 nmol: nanomole = 10 $^{-9}$ mol
- 5 fL: femtolitre = 10 $^{-15}$ L

1396 We consider isolated mitochondria as powerhouses and proton pumps as molecular
 1397 machines to relate experimental results to energy metabolism of the intact cell. The cellular
 1398 P_{\gg}/O_2 based on oxidation of glycogen is increased by the glycolytic (fermentative) substrate-
 1399 level phosphorylation of 3 $P_{\gg}/Glyc$, *i.e.*, 0.5 mol P_{\gg} for each mol O_2 consumed in the complete
 1400 oxidation of a mol glycosyl unit (Glyc). Adding 0.5 to the mitochondrial P_{\gg}/O_2 ratio of 5.4
 1401 yields a bioenergetic cell physiological P_{\gg}/O_2 ratio close to 6. Two NADH equivalents are
 1402 formed during glycolysis and transported from the cytosol into the mitochondrial matrix, either
 1403 by the malate-aspartate shuttle or by the glycerophosphate shuttle resulting in different
 1404 theoretical yield of ATP generated by mitochondria, the energetic cost of which potentially
 1405 must be taken into account. Considering also substrate-level phosphorylation in the TCA cycle,
 1406 this high P_{\gg}/O_2 ratio not only reflects proton translocation and OXPHOS studied in isolation,
 1407 but integrates mitochondrial physiology with energy transformation in the living cell (Gnaiger
 1408 1993a).

1409

1410 5. Conclusions

1411 MitoEAGLE can serve as a gateway to better diagnose mitochondrial respiratory defects
 1412 linked to genetic variation, age-related health risks, sex-specific mitochondrial performance,
 1413 lifestyle with its effects on degenerative diseases, and thermal and chemical environment. The
 1414 present recommendations on coupling control states and rates, linked to the concept of the
 1415 protonmotive force, are limited to studies with mitochondrial preparations. These will be
 1416 extended in a series of reports on pathway control of mitochondrial respiration, respiratory
 1417 states in intact cells, and harmonization of experimental procedures.

1418

1419 **Box 5: Mitochondrial and cell respiration**

1420 Mitochondrial and cell respiration is the process of highly exergonic and exothermic energy
 1421 transformation in which scalar redox reactions are coupled to vectorial ion translocation across
 1422 a semipermeable membrane, which separates the small volume of a bacterial cell or
 1423 mitochondrion from the larger volume of its surroundings. The electrochemical exergy can be
 1424 partially conserved in the phosphorylation of ADP to ATP or in ion pumping, or dissipated in
 1425 an electrochemical short-circuit. Respiration is thus clearly distinguished from fermentation as
 1426 the counterpart of cellular core energy metabolism. Respiration is separated in mitochondrial
 1427 preparations from the partial contribution of fermentative pathways of the intact cell. According
 1428 to this definition, residual oxygen consumption, as measured after inhibition of mitochondrial
 1429 electron transfer, does not belong to the class of catabolic reactions and is, therefore, subtracted
 1430 from total oxygen consumption to obtain baseline-corrected respiration.

1431

1432 The optimal choice for expressing mitochondrial and cell respiration (**Box 5**) as O_2 flow
 1433 per biological system, and normalization for specific tissue-markers (volume, mass, protein)
 1434 and mitochondrial markers (volume, protein, content, mtDNA, activity of marker enzymes,
 1435 respiratory reference state) is guided by the scientific question under study. Interpretation of
 1436 the obtained data depends critically on appropriate normalization, and therefore reporting rates
 1437 merely as $nmol \cdot s^{-1}$ is discouraged, since it restricts the analysis to intra-experimental
 1438 comparison of relative (qualitative) differences. Expressing O_2 consumption per cell may not
 1439 be possible when dealing with tissues. For studies with mitochondrial preparations, we
 1440 recommend that normalizations be provided as far as possible: (1) on a per cell basis as O_2 flow
 1441 (a biophysical normalization); (2) per g cell or tissue protein, or per cell or tissue mass as mass-
 1442 specific O_2 flux (a cellular normalization); and (3) per mitochondrial marker as mt-specific flux
 1443 (a mitochondrial normalization). With information on cell size and the use of multiple
 1444 normalizations, maximum potential information is available (Renner *et al.* 2003; Wagner *et al.*
 1445 2011; Gnaiger 2014). When using isolated mitochondria, mitochondrial protein is a frequently
 1446 applied mitochondrial marker, the use of which is basically restricted to isolated mitochondria.

1447 Mitochondrial markers, such as citrate synthase activity as an enzymatic matrix marker, provide
 1448 a link to the tissue of origin on the basis of calculating the mitochondrial yield, *i.e.*, the fraction
 1449 of mitochondrial marker obtained from a unit mass of tissue.

1450

1451 **Acknowledgements**

1452 We thank M. Beno for management assistance. Supported by COST Action CA15203
 1453 MitoEAGLE and K-Regio project MitoFit (EG).

1454

1455 **Competing financial interests:** E.G. is founder and CEO of Oroboros Instruments, Innsbruck,
 1456 Austria.

1457

1458 **6. References**

- 1459 Altmann R (1894) Die Elementarorganismen und ihre Beziehungen zu den Zellen. Zweite vermehrte Auflage.
 1460 Verlag Von Veit & Comp, Leipzig:160 pp.
- 1461 Beard DA (2005) A biophysical model of the mitochondrial respiratory system and oxidative phosphorylation.
 1462 PLoS Comput Biol 1(4):e36.
- 1463 Benda C (1898) Über die Spermatogenese der Vertebraten und höherer Evertebraten II Theil: Die Histogenese
 1464 der Spermien. Arch Anat Physiol 73:393-8.
- 1465 Birkedal R, Laasmaa M, Vendelin M (2014) The location of energetic compartments affects energetic
 1466 communication in cardiomyocytes. Front Physiol 5:376. doi: 10.3389/fphys.2014.00376. eCollection 2014.
- 1467 Breton S, Beaupré HD, Stewart DT, Hoeh WR, Blier PU (2007) The unusual system of doubly uniparental
 1468 inheritance of mtDNA: isn't one enough? Trends Genet 23:465-74.
- 1469 Brown GC (1992) Control of respiration and ATP synthesis in mammalian mitochondria and cells. Biochem J
 1470 284:1-13.
- 1471 Campos JC, Queliconi BB, Bozi LHM, Bechara LRG, Dourado PMM, Andres AM, Jannig PR, Gomes KMS,
 1472 Zambelli VO, Rocha-Resende C, Guatimosim S, Brum PC, Mochly-Rosen D, Gottlieb RA, Kowaltowski AJ,
 1473 Ferreira JCB (2017) Exercise reestablishes autophagic flux and mitochondrial quality control in heart failure.
 1474 Autophagy 13:1304-317.
- 1475 Chance B, Williams GR (1955a) Respiratory enzymes in oxidative phosphorylation. I. Kinetics of oxygen
 1476 utilization. J Biol Chem 217:383-93.
- 1477 Chance B, Williams GR (1955b) Respiratory enzymes in oxidative phosphorylation: III. The steady state. J Biol
 1478 Chem 217:409-27.
- 1479 Chance B, Williams GR (1955c) Respiratory enzymes in oxidative phosphorylation. IV. The respiratory chain. J
 1480 Biol Chem 217:429-38.
- 1481 Chance B, Williams GR (1956) The respiratory chain and oxidative phosphorylation. Adv Enzymol Relat Subj
 1482 Biochem 17:65-134.
- 1483 Cobb LJ, Lee C, Xiao J, Yen K, Wong RG, Nakamura HK, Mehta HH, Gao Q, Ashur C, Huffman DM, Wan J,
 1484 Muzumdar R, Barzilai N, Cohen P (2016) Naturally occurring mitochondrial-derived peptides are age-
 1485 dependent regulators of apoptosis, insulin sensitivity, and inflammatory markers. Aging (Albany NY) 8:796-
 1486 809.
- 1487 Cohen ER, Cvitas T, Frey JG, Holmström B, Kuchitsu K, Marquardt R, Mills I, Pavese F, Quack M, Stohner J,
 1488 Strauss HL, Takami M, Thor HL (2008) Quantities, units and symbols in physical chemistry, IUPAC Green
 1489 Book, 3rd Edition, 2nd Printing, IUPAC & RSC Publishing, Cambridge.
- 1490 Cooper H, Hedges LV, Valentine JC, eds (2009) The handbook of research synthesis and meta-analysis. Russell
 1491 Sage Foundation.
- 1492 Coopersmith J (2010) Energy, the subtle concept. The discovery of Feynman's blocks from Leibnitz to Einstein.
 1493 Oxford University Press:400 pp.
- 1494 Cummins J (1998) Mitochondrial DNA in mammalian reproduction. Rev Reprod 3:172-82.
- 1495 Dai Q, Shah AA, Garde RV, Yonish BA, Zhang L, Medvitz NA, Miller SE, Hansen EL, Dunn CN, Price TM
 1496 (2013) A truncated progesterone receptor (PR-M) localizes to the mitochondrion and controls cellular
 1497 respiration. Mol Endocrinol 27:741-53.
- 1498 Divakaruni AS, Brand MD (2011) The regulation and physiology of mitochondrial proton leak. Physiology
 1499 (Bethesda) 26:192-205.
- 1500 Doerrier C, Garcia-Souza LF, Krumschnabel G, Wohlfarter Y, Mészáros AT, Gnaiger E (2017) High-Resolution
 1501 FluoRespirometry and OXPHOS protocols for human cells, permeabilized fibres from small biopsies of
 1502 muscle and isolated mitochondria. Methods Mol. Biol. (in press)
- 1503 Doskey CM, van 't Erve TJ, Wagner BA, Buettner GR (2015) Moles of a substance per cell is a highly
 1504 informative dosing metric in cell culture. PLOS ONE 10:e0132572.

- 1505 Drahotka Z, Milerová M, Stieglerová A, Houstek J, Ostádal B (2004) Developmental changes of cytochrome *c*
 1506 oxidase and citrate synthase in rat heart homogenate. *Physiol Res* 53:119-22.
- 1507 Duarte FV, Palmeira CM, Rolo AP (2014) The role of microRNAs in mitochondria: small players acting wide.
 1508 *Genes (Basel)* 5:865-86.
- 1509 Dufour S, Rousse N, Canioni P, Diolez P (1996) Top-down control analysis of temperature effect on oxidative
 1510 phosphorylation. *Biochem J* 314:743-51.
- 1511 Ernster L, Schatz G (1981) Mitochondria: a historical review. *J Cell Biol* 91:227s-55s.
- 1512 Estabrook RW (1967) Mitochondrial respiratory control and the polarographic measurement of ADP:O ratios.
 1513 *Methods Enzymol* 10:41-7.
- 1514 Faber C, Zhu ZJ, Castellino S, Wagner DS, Brown RH, Peterson RA, Gates L, Barton J, Bickett M, Hagerty L,
 1515 Kimbrough C, Sola M, Bailey D, Jordan H, Elangbam CS (2014) Cardiolipin profiles as a potential
 1516 biomarker of mitochondrial health in diet-induced obese mice subjected to exercise, diet-restriction and
 1517 ephedrine treatment. *J Appl Toxicol* 34:1122-9.
- 1518 Fell D (1997) Understanding the control of metabolism. Portland Press.
- 1519 Garlid KD, Beavis AD, Ratkje SK (1989) On the nature of ion leaks in energy-transducing membranes. *Biochim*
 1520 *Biophys Acta* 976:109-20.
- 1521 Garlid KD, Semrad C, Zinchenko V. Does redox slip contribute significantly to mitochondrial respiration? In:
 1522 Schuster S, Rigoulet M, Ouhabi R, Mazat J-P, eds (1993) Modern trends in biothermokinetics. Plenum Press,
 1523 New York, London:287-93.
- 1524 Gerö D, Szabo C (2016) Glucocorticoids suppress mitochondrial oxidant production via upregulation of
 1525 uncoupling protein 2 in hyperglycemic endothelial cells. *PLoS One* 11:e0154813.
- 1526 Gibney E (2017) New definitions of scientific units are on the horizon. *Nature* 550:312–13.
- 1527 Gnaiger E. Efficiency and power strategies under hypoxia. Is low efficiency at high glycolytic ATP production a
 1528 paradox? In: Surviving Hypoxia: Mechanisms of Control and Adaptation. Hochachka PW, Lutz PL, Sick T,
 1529 Rosenthal M, Van den Thillart G, eds (1993a) CRC Press, Boca Raton, Ann Arbor, London, Tokyo:77-109.
- 1530 Gnaiger E (1993b) Nonequilibrium thermodynamics of energy transformations. *Pure Appl Chem* 65:1983-2002.
- 1531 Gnaiger E (2001) Bioenergetics at low oxygen: dependence of respiration and phosphorylation on oxygen and
 1532 adenosine diphosphate supply. *Respir Physiol* 128:277-97.
- 1533 Gnaiger E (2009) Capacity of oxidative phosphorylation in human skeletal muscle. New perspectives of
 1534 mitochondrial physiology. *Int J Biochem Cell Biol* 41:1837-45.
- 1535 Gnaiger E (2014) Mitochondrial pathways and respiratory control. An introduction to OXPHOS analysis. 4th ed.
 1536 *Mitochondr Physiol Network* 19.12. Oroboros MiPNet Publications, Innsbruck:80 pp.
- 1537 Gnaiger E, Méndez G, Hand SC (2000) High phosphorylation efficiency and depression of uncoupled respiration
 1538 in mitochondria under hypoxia. *Proc Natl Acad Sci USA* 97:11080-5.
- 1539 Greggio C, Jha P, Kulkarni SS, Lagarrigue S, Broskey NT, Boutant M, Wang X, Conde Alonso S, Ofori E,
 1540 Auwerx J, Cantó C, Amati F (2017) Enhanced respiratory chain supercomplex formation in response to
 1541 exercise in human skeletal muscle. *Cell Metab* 25:301-11.
- 1542 Hofstadter DR (1979) Gödel, Escher, Bach: An eternal golden braid. A metaphorical fugue on minds and
 1543 machines in the spirit of Lewis Carroll. Harvester Press:499 pp.
- 1544 Illaste A, Laasmaa M, Peterson P, Vendelin M (2012) Analysis of molecular movement reveals latticelike
 1545 obstructions to diffusion in heart muscle cells. *Biophys J* 102:739-48.
- 1546 Jasienski M, Bazzaz FA (1999) The fallacy of ratios and the testability of models in biology. *Oikos* 84:321-26.
- 1547 Jepihhina N, Beraud N, Sepp M, Birkedal R, Vendelin M (2011) Permeabilized rat cardiomyocyte response
 1548 demonstrates intracellular origin of diffusion obstacles. *Biophys J* 101:2112-21.
- 1549 Klepinin A, Ounpuu L, Guzun R, Chekulayev V, Timohhina N, Tepp K, Shevchuk I, Schlattner U, Kaambre T
 1550 (2016) Simple oxygraphic analysis for the presence of adenylate kinase 1 and 2 in normal and tumor cells. *J*
 1551 *Bioenerg Biomembr* 48:531-48.
- 1552 Klingenberg M (2017) UCP1 - A sophisticated energy valve. *Biochimie* 134:19-27.
- 1553 Koit A, Shevchuk I, Ounpuu L, Klepinin A, Chekulayev V, Timohhina N, Tepp K, Puurand M, Truu L, Heck K,
 1554 Valvere V, Guzun R, Kaambre T (2017) Mitochondrial respiration in human colorectal and breast cancer
 1555 clinical material is regulated differently. *Oxid Med Cell Longev* 1372640.
- 1556 Komlódi T, Tretter L (2017) Methylene blue stimulates substrate-level phosphorylation catalysed by succinyl-
 1557 CoA ligase in the citric acid cycle. *Neuropharmacology* 123:287-98.
- 1558 Lane N (2005) Power, sex, suicide: mitochondria and the meaning of life. Oxford University Press:354 pp.
- 1559 Larsen S, Nielsen J, Neigaard Nielsen C, Nielsen LB, Wibrand F, Stride N, Schroder HD, Boushel RC, Helge
 1560 JW, Dela F, Hey-Mogensen M (2012) Biomarkers of mitochondrial content in skeletal muscle of healthy
 1561 young human subjects. *J Physiol* 590:3349-60.
- 1562 Lee C, Zeng J, Drew BG, Sallam T, Martin-Montalvo A, Wan J, Kim SJ, Mehta H, Hevener AL, de Cabo R,
 1563 Cohen P (2015) The mitochondrial-derived peptide MOTS-c promotes metabolic homeostasis and reduces
 1564 obesity and insulin resistance. *Cell Metab* 21:443-54.

- 1565 Lee SR, Kim HK, Song IS, Youm J, Dizon LA, Jeong SH, Ko TH, Heo HJ, Ko KS, Rhee BD, Kim N, Han J
 1566 (2013) Glucocorticoids and their receptors: insights into specific roles in mitochondria. *Prog Biophys Mol*
 1567 *Biol* 112:44-54.
- 1568 Leek BT, Mudaliar SR, Henry R, Mathieu-Costello O, Richardson RS (2001) Effect of acute exercise on citrate
 1569 synthase activity in untrained and trained human skeletal muscle. *Am J Physiol Regul Integr Comp Physiol*
 1570 280:R441-7.
- 1571 Lemieux H, Blier PU, Gnaiger E (2017) Remodeling pathway control of mitochondrial respiratory capacity by
 1572 temperature in mouse heart: electron flow through the Q-junction in permeabilized fibers. *Sci Rep* 7:2840.
- 1573 Lenaz G, Tioli G, Falasca AI, Genova ML (2017) Respiratory supercomplexes in mitochondria. In: *Mechanisms*
 1574 *of primary energy transduction in biology*. M Wikstrom (ed) Royal Society of Chemistry Publishing, London,
 1575 UK:296-337.
- 1576 Margulis L (1970) *Origin of eukaryotic cells*. New Haven: Yale University Press.
- 1577 Meinild Lundby AK, Jacobs RA, Gehrig S, de Leur J, Hauser M, Bonne TC, Flück D, Dandanell S, Kirk N,
 1578 Kaech A, Ziegler U, Larsen S, Lundby C (2017) Exercise training increases skeletal muscle mitochondrial
 1579 volume density by enlargement of existing mitochondria and not de novo biogenesis. *Acta Physiol (Oxf)*
 1580 [Epub ahead of print].
- 1581 Menshikova EV, Ritov VB, Fairfull L, Ferrell RE, Kelley DE, Goodpaster BH (2006) Effects of exercise on
 1582 mitochondrial content and function in aging human skeletal muscle. *J Gerontol A Biol Sci Med Sci* 61:534-
 1583 40.
- 1584 Menshikova EV, Ritov VB, Ferrell RE, Azuma K, Goodpaster BH, Kelley DE (2007) Characteristics of skeletal
 1585 muscle mitochondrial biogenesis induced by moderate-intensity exercise and weight loss in obesity. *J Appl*
 1586 *Physiol* (1985) 103:21-7.
- 1587 Menshikova EV, Ritov VB, Toledo FG, Ferrell RE, Goodpaster BH, Kelley DE (2005) Effects of weight loss
 1588 and physical activity on skeletal muscle mitochondrial function in obesity. *Am J Physiol Endocrinol Metab*
 1589 288:E818-25.
- 1590 Miller GA (1991) *The science of words*. Scientific American Library New York:276 pp. Mitchell P (1961)
 1591 Coupling of phosphorylation to electron and hydrogen transfer by a chemi-osmotic type of mechanism.
 1592 *Nature* 191:144-8.
- 1593 Mitchell P (2011) Chemiosmotic coupling in oxidative and photosynthetic phosphorylation. *Biochim Biophys*
 1594 *Acta Bioenergetics* 1807:1507-38.
- 1595 Mitchell P, Moyle J (1967) Respiration-driven proton translocation in rat liver mitochondria. *Biochem J*
 1596 105:1147-62.
- 1597 Mogensen M, Sahlin K, Fernström M, Glinborg D, Vind BF, Beck-Nielsen H, Højlund K (2007) Mitochondrial
 1598 respiration is decreased in skeletal muscle of patients with type 2 diabetes. *Diabetes* 56:1592-9.
- 1599 Moreno M, Giacco A, Di Munno C, Goglia F (2017) Direct and rapid effects of 3,5-diiodo-L-thyronine (T2).
 1600 *Mol Cell Endocrinol* 7207:30092-8.
- 1601 Morrow RM, Picard M, Derbeneva O, Leipzig J, McManus MJ, Gousspillou G, Barbat-Artigas S, Dos Santos C,
 1602 Hepple RT, Murdock DG, Wallace DC (2017) Mitochondrial energy deficiency leads to hyperproliferation of
 1603 skeletal muscle mitochondria and enhanced insulin sensitivity. *Proc Natl Acad Sci U S A* 114:2705-10.
- 1604 Paradies G, Paradies V, De Benedictis V, Ruggiero FM, Petrosillo G (2014) Functional role of cardiolipin in
 1605 mitochondrial bioenergetics. *Biochim Biophys Acta* 1837:408-17.
- 1606 Pesta D, Hoppel F, Macek C, Messner H, Faulhaber M, Kobel C, Parson W, Burtcher M, Schocke M, Gnaiger
 1607 E (2011) Similar qualitative and quantitative changes of mitochondrial respiration following strength and
 1608 endurance training in normoxia and hypoxia in sedentary humans. *Am J Physiol Regul Integr Comp Physiol*
 1609 301:R1078-87.
- 1610 Price TM, Dai Q (2015) The role of a mitochondrial progesterone receptor (PR-M) in progesterone action.
 1611 *Semin Reprod Med* 33:185-94.
- 1612 Prigogine I (1967) *Introduction to thermodynamics of irreversible processes*. Interscience, New York, 3rd
 1613 ed:147pp.
- 1614 Puchowicz MA, Varnes ME, Cohen BH, Friedman NR, Kerr DS, Hoppel CL (2004) Oxidative phosphorylation
 1615 analysis: assessing the integrated functional activity of human skeletal muscle mitochondria – case studies.
 1616 *Mitochondrion* 4:377-85. Puntchart A, Claassen H, Jostardt K, Hoppeler H, Billeter R (1995) mRNAs of
 1617 enzymes involved in energy metabolism and mtDNA are increased in endurance-trained athletes. *Am J*
 1618 *Physiol* 269:C619-25.
- 1619 Quiros PM, Mottis A, Auwerx J (2016) Mitonuclear communication in homeostasis and stress. *Nat Rev Mol*
 1620 *Cell Biol* 17:213-26.
- 1621 Reichmann H, Hoppeler H, Mathieu-Costello O, von Bergen F, Pette D (1985) Biochemical and ultrastructural
 1622 changes of skeletal muscle mitochondria after chronic electrical stimulation in rabbits. *Pflugers Arch* 404:1-
 1623 9.
- 1624 Renner K, Amberger A, Konwalinka G, Gnaiger E (2003) Changes of mitochondrial respiration, mitochondrial
 1625 content and cell size after induction of apoptosis in leukemia cells. *Biochim Biophys Acta* 1642:115-23.
- 1626 Rich P (2003) Chemiosmotic coupling: The cost of living. *Nature* 421:583.

- 1627 Rostovtseva TK, Sheldon KL, Hassanzadeh E, Monge C, Saks V, Bezrukov SM, Sackett DL (2008) Tubulin
1628 binding blocks mitochondrial voltage-dependent anion channel and regulates respiration. *Proc Natl Acad Sci*
1629 *USA* 105:18746-51.
- 1630 Rustin P, Parfait B, Chretien D, Bourgeron T, Djouadi F, Bastin J, Rötig A, Munnich A (1996) Fluxes of
1631 nicotinamide adenine dinucleotides through mitochondrial membranes in human cultured cells. *J Biol Chem*
1632 271:14785-90.
- 1633 Saks VA, Veksler VI, Kuznetsov AV, Kay L, Sikk P, Tiivel T, Tranqui L, Olivares J, Winkler K, Wiedemann F,
1634 Kunz WS (1998) Permeabilised cell and skinned fiber techniques in studies of mitochondrial function in
1635 vivo. *Mol Cell Biochem* 184:81-100.
- 1636 Salabei JK, Gibb AA, Hill BG (2014) Comprehensive measurement of respiratory activity in permeabilized cells
1637 using extracellular flux analysis. *Nat Protoc* 9:421-38.
- 1638 Sazanov LA (2015) A giant molecular proton pump: structure and mechanism of respiratory complex I. *Nat Rev*
1639 *Mol Cell Biol* 16:375-88.
- 1640 Schneider TD (2006) Claude Shannon: biologist. The founder of information theory used biology to formulate
1641 the channel capacity. *IEEE Eng Med Biol Mag* 25:30-3.
- 1642 Schönfeld P, Dymkowska D, Wojtczak L (2009) Acyl-CoA-induced generation of reactive oxygen species in
1643 mitochondrial preparations is due to the presence of peroxisomes. *Free Radic Biol Med* 47:503-9.
- 1644 Schrödinger E (1944) *What is life? The physical aspect of the living cell.* Cambridge Univ Press.
- 1645 Schultz J, Wiesner RJ (2000) Proliferation of mitochondria in chronically stimulated rabbit skeletal muscle--
1646 transcription of mitochondrial genes and copy number of mitochondrial DNA. *J Bioenerg Biomembr* 32:627-
1647 34.
- 1648 Simson P, Jepihhina N, Laasmaa M, Peterson P, Birkedal R, Vendelin M (2016) Restricted ADP movement in
1649 cardiomyocytes: Cytosolic diffusion obstacles are complemented with a small number of open mitochondrial
1650 voltage-dependent anion channels. *J Mol Cell Cardiol* 97:197-203.
- 1651 Stucki JW, Ineichen EA (1974) Energy dissipation by calcium recycling and the efficiency of calcium transport
1652 in rat-liver mitochondria. *Eur J Biochem* 48:365-75.
- 1653 Tonkonogi M, Harris B, Sahlin K (1997) Increased activity of citrate synthase in human skeletal muscle after a
1654 single bout of prolonged exercise. *Acta Physiol Scand* 161:435-6.
- 1655 Waczulikova I, Habodaszova D, Cagalinec M, Ferko M, Ulicna O, Mateasik A, Sikurova L, Ziegelhöffer A
1656 (2007) Mitochondrial membrane fluidity, potential, and calcium transients in the myocardium from acute
1657 diabetic rats. *Can J Physiol Pharmacol* 85:372-81.
- 1658 Wagner BA, Venkataraman S, Buettner GR (2011) The rate of oxygen utilization by cells. *Free Radic Biol Med*
1659 51:700-712.
- 1660 Wang H, Hiatt WR, Barstow TJ, Brass EP (1999) Relationships between muscle mitochondrial DNA content,
1661 mitochondrial enzyme activity and oxidative capacity in man: alterations with disease. *Eur J Appl Physiol*
1662 *Occup Physiol* 80:22-7.
- 1663 Wang T (2010) Coulomb force as an entropic force. *Phys Rev D* 81:104045.
- 1664 Watt IN, Montgomery MG, Runswick MJ, Leslie AG, Walker JE (2010) Bioenergetic cost of making an
1665 adenosine triphosphate molecule in animal mitochondria. *Proc Natl Acad Sci U S A* 107:16823-7.
- 1666 Weibel ER, Hoppeler H (2005) Exercise-induced maximal metabolic rate scales with muscle aerobic capacity. *J*
1667 *Exp Biol* 208:1635-44.
- 1668 White DJ, Wolff JN, Pierson M, Gemmell NJ (2008) Revealing the hidden complexities of mtDNA inheritance.
1669 *Mol Ecol* 17:4925-42.
- 1670 Wikström M, Hummer G (2012) Stoichiometry of proton translocation by respiratory complex I and its
1671 mechanistic implications. *Proc Natl Acad Sci U S A* 109:4431-6.
- 1672 Willis WT, Jackman MR, Messer JI, Kuzmiak-Glancy S, Glancy B (2016) A simple hydraulic analog model of
1673 oxidative phosphorylation. *Med Sci Sports Exerc* 48:990-1000.